ANALYSIS OF A DYNAMICAL SYSTEM OF ANIMAL GROWTH AND COMPOSITION.

A thesis submitted in partial fulfilment of the requirements for the degree of

Master of Science

in

Mathematics.

at Massey University, Albany,

New Zealand.

Nurul Syaza Abdul Latif

2010

ABSTRACT

This thesis investigates the analysis of the extended model of animal growth proposed by Oliviera *et al* (personal communication, July 2009). This mechanistic model of animal growth based on a detailed representation of energy dynamics focussing on the interaction between four compartment of body composition; nutrient level, fat content, visceral protein and non-visceral protein. The model is mathematically analysed and the behaviour of the model for different feeding level is examined. The animal growth model exhibits thresholds typical of nonlinear systems and multiple stable steady states which have distinct basins of stability which depend on the value of the large number of physiologically-determined parameters. These have not been previously explored theoretically and these are done in this thesis. The model demonstrates richer behaviour where path-following techniques are used to explore the distribution in parameter space of the varying phenomenology.

ACKNOWLEDGEMENT

I owe my deepest gratitude to my supervisor, Professor Graeme Wake, whose encouragement, guidance and support from the initial to the final level enabled me to develop an understanding of the subject. Not to forget, my co-supervisor, Dr. Kumar Vetharaniam (AgResearch), for giving me the opportunity to do this project. It has been a great pleasure to work with both of them.

Lastly, I offer my regards and blessings to all of those who supported me in any respect during the completion of the project.

TABLE OF CONTENTS

LIST OF FIGURES

LIST OF TABLES

CHAPTER 1

INTRODUCTION

In this chapter, we briefly discuss the background of this study. Also, we mention the scope and objectives of the project.

1.1 Background of the study

For most discussions, growth may be defined as the progressive increase in the size (volume, length or height) or weight of an animal over time. Hence, growth results from the accretion of nutrients over time. Animal growth is best described by taking measurements of the physical characteristics of the animal (weight, height or length) or attributes of a tissue (back fat thickness and muscle depth) or even a portion of the animal, such as noting changes in the length of a limb as the animal progresses from neonate (a newborn animal) to maturity.

The understanding of the biology of animal growth has lead to opportunities for improving the efficiency and quality of animal production. Such opportunities depend on

the ability to control and predict the outcome in animal feeding and management. This requires the development and use of mathematical models of growth. The mathematical representation and prediction of growth has been a widespread endeavour in biology and a wide range of approaches have been proposed. A number of equations have been used to represent growth of an animal and its body components. These include the exponential, logistic, Brody, Gompertz and Richardson functions and many others (France and Kebreab, 2008).

Nutritional models for growing animals should enable accurate predictions of nutrient requirements, calculations of responses of defined animals to defined feeds and calculation of optimal nutritional strategies. Feeding systems based upon these models typically handle the consumption of energy, protein and other nutrients separately. However, there is lack of information and some indications on the relationship between nutrition and reproduction. A model that has been developed by Oliviera *et al* (personal communication, July 2009), proposed a closer investigation on the effect of energy and protein mobilization on days to first ovulation in early lactation dairy cows. For this project, we expand and analyse this energetic model of growth that can trace the effects of alternate nutritional strategies on animal performance, energy and protein requirements through time.

1.2 Scope and Objectives of the Study

Over the last decade, there has been an increasing use of the models in animal growth research, both independently and in conjunction with experimental work. The model presented here has been developed by Oliviera *et al* but not yet published (personal communication, July 2009). We scope the proposed model as an autonomous dynamical system. The animal model described here draws from a wide range of sources in the literature and the parameterisation has been done before by Oliviera *et al*.

The following are the objectives of the study:-

i. To expand the existing energetic model of growth in the dairy cow (Oliviera *et al*).
ii. To explore the dynamics of the interacting pools (nutrient, protein, viscera, fat).
iii. To analyse behaviour and determine the steady-state stability.
iv. To demonstrate bifurcation diagrams and analyse the biological interpretation behind those diagrams.

CHAPTER 2

MATHEMATICAL THEORY

In this chapter, we discuss some mathematical theories that are related with this project.

2.1 Animal Growth Model as a Dynamical System

Traditionally, quantitative research into animal growth or animal nutrient, as in many other areas of biology, has been empirically based and has centred on statistical analysis of experimental work. While this has provided much of the essential groundwork, more attention has been given in recent years to improving understanding of the underlying mechanisms that govern the process of digestion. This requires an increased emphasis on theory and mathematical modelling.

The term dynamic is self explanatory. Dynamics models are based upon differential equations of the form

$$\frac{d\boldsymbol{x}}{dt} = \boldsymbol{f}(t, \boldsymbol{x}, \lambda) \tag{2.1}$$

The model consists of a number of state variables, $\boldsymbol{x} = (x_1, x_2, ..., x_n)$, that represent the essential characteristics we are trying to examine under the model. These equations, $\boldsymbol{f} = (f_1, f_2, \ldots, f_n)$, will include a number of parameters (e.g. λ) of the system that are arbitrary constant.

One or more of these parameters may define something that can be controlled. In a system describing animal growth, for example, we can control the amount of feeding. If we choose to do this, we then can identify the amount of feeding as a control parameter. We can investigate how the model changes when the control parameter is changed. The choice of control parameter does not change the construction of the model. It does, however, verify how we will analyse the model.

A solution to the model is a curve that satisfies the differential equation for all values of the independent variable. These solutions may be found analytically and are integrated over time, usually using a numerical integration technique such as *Runge-Kutta Methods*. A solution of a model represents the evolution of the animal as time progresses.

Up to this point for this project, we only considered autonomous dynamical systems, that is, a system of differential equations which does not depend explicitly on the independent variable, *t*.

$$\frac{d\boldsymbol{x}}{dt} = \boldsymbol{f}(\boldsymbol{x}, \lambda) \tag{2.2}$$

However, a non-autonomous dynamical system, $\boldsymbol{f}$ is explicitly dependent on variable time *t*. Non-autonomous systems are much more difficult to characterise than autonomous ones unless it has a particularly simple structure.

2.1.1 Structural Stability

In mathematics, structural stability is a fundamental property of a dynamical system, which means that the qualitative behaviour of the trajectories (or vector field) is unaffected by small perturbations.

Definition: The direction field or *vector field* gives the gradients $\frac{d\boldsymbol{x}}{dt}$ and direction vectors of the trajectories in the phase plane.

Structural stability of the system provides a justification for applying the qualitative theory of dynamical systems to analysis of concrete physical systems.

If we try to model physical systems that demonstrate structural stability, then provided we put up a model that approximates the system closely enough, the result will be quantitatively the same. Similarly, if the model is structurally stable, then a small variation

to the parameter values will not change the system qualitatively, nor will additional small, non-linear terms. This is attention-grabbing when considering a model of a physical system, since if the model is not structurally stable, then it may be vulnerable to the changes in the parameter values. These parameter values may have been obtained by experiment and thus have experimental error associated with them. So if a system is not structurally stable, there would be no repeatable pattern to observe.

2.1.2 Types of Steady State

In general, a steady state is a point that does not change upon application of a map, system of differential equation, etc. In particular, consider an autonomous system of ordinary differential equations (ODEs) at which the functions are continuously differentiable

$$\begin{cases} \dfrac{dx_1}{dt} = f_1(x_1,\ldots,x_n) = 0 \\ \vdots \\ \dfrac{dx_n}{dt} = f_n(x_1,\ldots,x_n) = 0 \end{cases} . \qquad (2.3)$$

These points are known as steady state points.

If a variable is slightly displaced from a steady state point, it may:-

1. Move back to the steady state point– attractor ("asymptotically stable" or "superstable"),
2. Move away – repellor ("unstable"),

3. Move in a neighbourhood of the fixed point but not approach it ("stable" but not "asymptotically stable").

Steady state points are also known as critical points or equilibrium points. If a variable starts at a point that is not a steady state point, it cannot reach a steady state point in a finite amount of time. Also, a trajectory passing through at least one point that is not a steady state point cannot cross itself unless it is a closed curve, in which case it corresponds to a periodic solution.

The following equations and table summarizes types of possible steady states for a two-dimensional system (Tabor 1989).

1. If $\lambda_1 \neq \lambda_2$, then $\delta \boldsymbol{X} = c_1 \boldsymbol{D}_1 e^{\lambda_1 t} + c_2 \boldsymbol{D}_2 e^{\lambda_2 t}$

2. If $\lambda_1 = \lambda_2$, then $\delta \boldsymbol{X} = \left(c_1 \boldsymbol{D}_1 + c_2 \left(\boldsymbol{D}_1 + \boldsymbol{D}_2 t\right)\right) e^{\lambda t}$

λ	**Steady state**
$\lambda_1 < \lambda_2 < 0$	stable node
$\lambda_1 > \lambda_2 > 0$	unstable node
$\lambda_1 < 0 < \lambda_2$	hyperbolic fixed point
$\lambda_{1,2} = -\alpha \pm i\,\beta$	stable spiral point
$\lambda_{1,2} = \alpha \pm i\,\beta$	unstable spiral point
$\lambda_{1,2} = \pm i\,\omega$	elliptic fixed point
$\lambda_1 = \lambda_2 < 0$, if $\mathbf{D_1}$ is arbitrary and $\mathbf{D_2}$ is a null vector	stable star

$\lambda_1 = \lambda_2 > 0$, if $\mathbf{D_1}$ is arbitrary and $\mathbf{D_2}$ is a null vector	unstable star
$\lambda_1 = \lambda_2 < 0$, if $\mathbf{D_1}$ is arbitrary and $\mathbf{D_2}$ is not a null vector	stable improper node
$\lambda_1 = \lambda_2 > 0$, if $\mathbf{D_1}$ is arbitrary and $\mathbf{D_2}$ is not a null vector	unstable improper node

Table 2.1: Types of steady state.

Here $\delta \boldsymbol{X}$ is the column vector, λ is eigenvalue, and **D** is eigenvector and $\alpha, \beta, \omega \in \Re$.

In general, for the stability, the eigenvalues λ_i of a $n \times n$ matrix, *A*, are given by the characteristic equation $\det(A - \lambda I) = 0$; *I* is the identity matrix. For a nonlinear system, *A* is the Jacobian matrix evaluated at the steady state point.

1. For all $\mathrm{Re}(\lambda_i) < 0$, then the steady state is stable.
2. If there exists an eigenvalue λ such that $\mathrm{Re}(\lambda) > 0$, then the steady state is unstable.
3. If there exists an eigenvalue λ with $\mathrm{Re}(\lambda) = 0$ and all other $\mathrm{Re}(\lambda) < 0$, then the linearised system is neutrally stable and the stability of the nonlinear system is determined by the higher order terms.

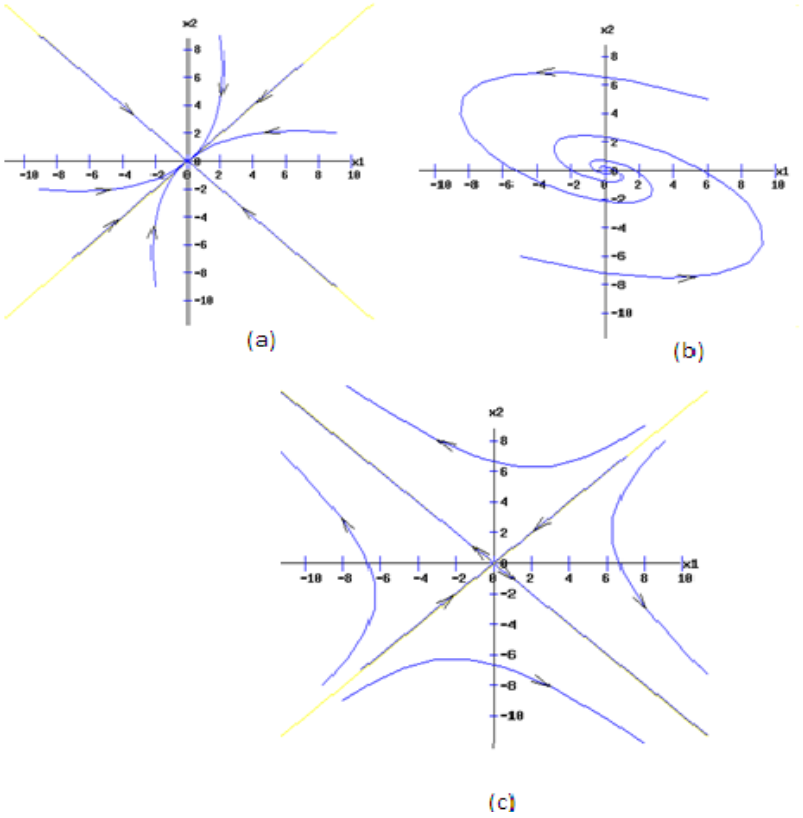

Figure 2.1: Different types of steady state (in two-dimensions) at the origin.
(a) a node, (b) a stable spiral and (c) a saddle.

Note that in the phase diagrams are for the linearised situation and the behaviour is as shown in the Figure 2.1 only in the neighbourhood of the origin. The global behaviour is more complicated of course.

Definition: If $\bar{\boldsymbol{x}}$ be the steady state points of the system (i.e. $\frac{d\boldsymbol{x}}{dt} = \boldsymbol{f}(\boldsymbol{x}, \lambda) = \boldsymbol{0}$), then the basin of attraction is the set of initial conditions $\boldsymbol{x}_0$ such that $\boldsymbol{x}(t) \to \bar{\boldsymbol{x}}$ as $t \to \infty$.

A *centre* is neither stable nor unstable. A system containing a centre is structurally unstable. It is the change between a stable spiral and unstable spiral, and neither attracts nor repels. It may be associated with an infinite number of periodic solutions nearby.

2.1.3 Bifurcation Theory

Bifurcation theory is the mathematical study of changes in the qualitative or topological structure of the solution of a family of differential equations. If the behaviour of a dynamical system changes suddenly as a parameter is varied, then it is said to have undergone bifurcation. At a point of bifurcation, stability may be gained or lost. Bifurcations are important scientifically because they provide models of transitions and instabilities as some control parameter is varied. It may be possible for a nonlinear system to have more than one steady state solution. For example, different initial conditions can lead to different stable solutions. A system of this form is said to be multiple stability.

Definition: An autonomous dynamical system

$$\frac{d\boldsymbol{x}}{dt} = \boldsymbol{f}(\boldsymbol{x}, \lambda)$$

is said to be *multiple stability* if there is more than one possible steady state solution for a fixed value of the parameter λ. The steady state obtained depends on the initial conditions.

The existence of multiple stability solutions allows for the possibility of bi-stability (*hysteresis*) as a parameter is varied. The two essential ingredients for bi-stability

behaviour are nonlinearity and feedback. To create a bi-stability region there must be some history in the system or depends on the initial conditions of the system.

Definition: An autonomous dynamical system

$$\frac{d\boldsymbol{x}}{dt} = \boldsymbol{f}(\boldsymbol{x}, \lambda)$$

has a *bi-stability* solution if there are two stable steady states for a fixed but arbitrarily parameter λ and the steady state obtained depends on the initial conditions.

Bifurcations come in two different categories:-

1. Global bifurcations – which often occur when larger invariant sets of the system 'collide' with each other or with steady states of the system. This type of bifurcation cannot be detected solely by a stability analysis of the steady state.

2. Local bifurcations – which can be analysed entirely through changes in the local stability properties of steady state, periodic orbits or other invariant sets.

Global bifurcations

This kind of bifurcation occurs when 'larger' invariant sets, such as periodic orbits, collide with the fixed point. This causes changes in the topology of the trajectories (the graphical behaviour) in the phase space which cannot be confined to a small neighbourhood, as is the case with local bifurcations. Moreover, the changes in topology extend out to an arbitrarily larger distance. Hence it is called global bifurcation.

Examples of global bifurcation:-

- Homoclinic bifurcation – in which a limit cycle collides with a saddle point
- Heteroclinic bifurcation – in which a limit cycle collides with two or more saddle points.
- Infinite-period bifurcation – a stable node and saddle point occur simultaneously on a limit cycle.
- Blue-sky catastrophe – in which a limit cycle collides with a non-hyperbolic cycle.

Global bifurcation can also involve more complicated sets such as chaotic attractors.

Local Bifurcations

A local bifurcation is occurring when the stability of the steady state point is changed when the parameter value is varied. In continuous systems, this corresponds to the real part of an eigenvalue of a steady state point passing through zero where the steady state is non-hyperbolic at the bifurcation point. The topological changes in the phase portrait of the system can be limited to arbitrarily small neighbourhoods of the bifurcating steady state points by moving the bifurcation parameter close to the bifurcation point. That is why it is called local bifurcation.

More theoretically, consider a continuous dynamical system described by the autonomous ordinary differential equations (ODEs)

$$\frac{d\boldsymbol{x}}{dt} = \boldsymbol{f}(\boldsymbol{x}, \lambda) \quad ; \quad \boldsymbol{f}: \Re^n \times \Re \to \Re^n . \tag{2.4}$$

The necessary condition of a local bifurcation of steady state occurs at $(\bar{\boldsymbol{x}}, \lambda_0)$ if the Jacobian matrix, $\left.\frac{d\boldsymbol{f}}{d\boldsymbol{x}}\right|_{(\bar{\boldsymbol{x}},\lambda_0)}$, has a zero eigenvalue. The sufficient condition is when the algebraic multiplicity of the zero eigenvalue is odd. This is made clear in Temme (1978). If the (two) eigenvalues are purely imaginary, it can be a Hopf bifurcation, with the appearance of periodic solutions. We have to note that the complex eigenvalues occur in the complex conjugate pairs.

Illustrations of local bifurcations:-

- Saddle-node bifurcation
- Transcritical bifurcation
- Pitchfork bifurcation
- Hopf bifurcation

Saddle-Node Bifurcation

The saddle-node bifurcation occurs when the steady state points are formed and destroyed. For example, as we varied a parameter, two steady state points moving towards each other collide and mutually annihilate.

Example: $\frac{dx}{dt} = \lambda + x^2$ (2.5)

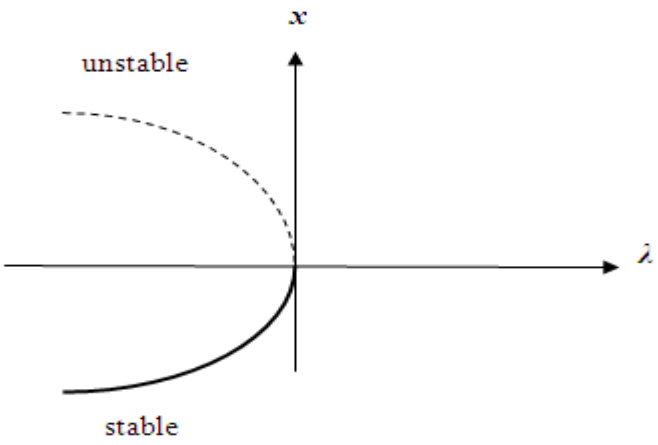

Figure 2.2: An example of saddle-node bifurcation.

The steady state point is defined by $\frac{dx}{dt} = 0$ is $x^2 = -\lambda$. The origin $(x, \lambda) = (0,0)$ is the bifurcation point, where the stable and unstable branches adhere, resulting in an exchange of stability.

Sometimes a saddle-node bifurcation is called a fold bifurcation or a turning-point bifurcation. Abraham and Shaw (1988) wrote the most inventive terminology for saddle-node bifurcation, which is *blue sky bifurcation*.

Transcritical Bifurcation

There are some certain scientific situations where a steady state point must exist for all values of a parameter and never be destroyed. But if we vary the parameter values, the steady state point will change its stability. The transcritical bifurcation is the standard mechanism for such changes in stability.

Example: $\frac{dx}{dt} = \lambda x - x^2$ (2.6)

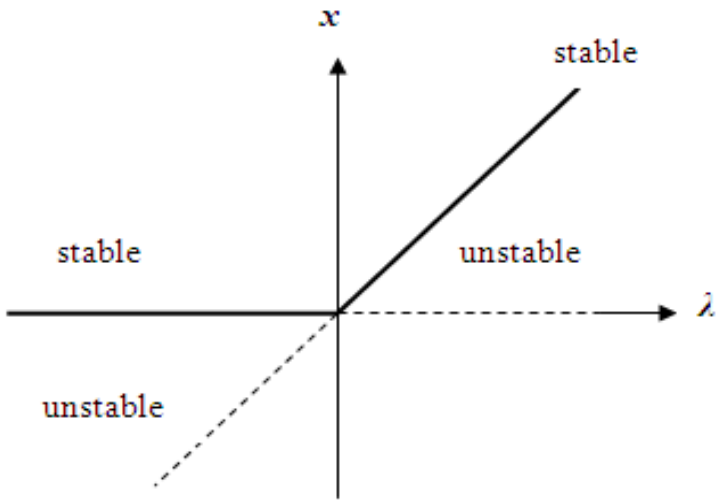

Figure 2.3: An example of transcritical bifurcation.

The steady state points are $\bar{x} = 0, \lambda$ obtained by solving $\frac{dx}{dt} = 0$. The origin is the bifurcation point where two branches intersect and exchange stability at $\bar{x}_1 = 0$ for all values of λ with $\lambda < 0$ stable and $\lambda > 0$ unstable. While, at $\bar{x}_2 = \lambda$ branch, it is stable on the first quadrant and it is unstable on the third quadrant.

Pitchfork Bifurcation

This bifurcation is common in physical problem that has a symmetry. There are problems that have a spatial symmetry between left and right. In such cases, the steady state points tend to appear and disappear in symmetrical pairs. There are two very different

types of pitchfork bifurcation; supercritical pitchfork and subcritical pitchfork. In the engineering literature, supercritical pitchfork bifurcations are sometimes called soft (or safe). The amplitude of the limit cycle builds up gradually as the parameter is moved away from the bifurcation point. In contrast, subcritical pitchfork bifurcations are hard (or dangerous). A steady state, say, at the origin, could become unstable as a parameter varies and the nonzero solutions could tend to infinity.

i) Supercritical Pitchfork Bifurcation

The normal form of the supercritical pitchfork bifurcation is

Example: $\frac{dx}{dt} = \lambda x - x^3$ (2.7)

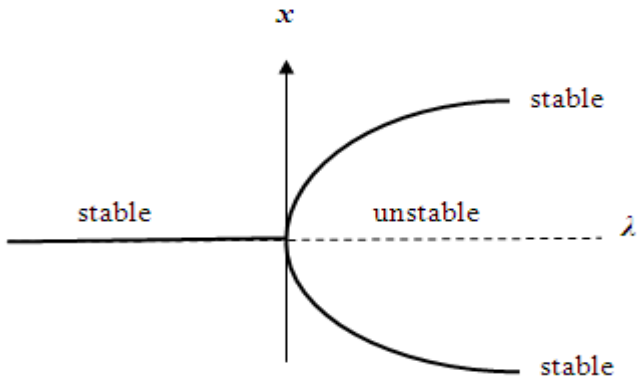

Figure 2.4: An example of supercritical pitchfork bifurcation.

When $\lambda < 0$, the steady state point at $\bar{x} = 0$ is stable. When $\lambda = 0$, the steady state point is still stable. When $\lambda > 0$, the steady state point becomes unstable. There exist two new stable steady states on either side of the origin, symmetrically located at $\pm\sqrt{\lambda}$.

ii) Subcritical Pitchfork Bifurcation

The normal form of the subcritical pitchfork bifurcation

Example: $\frac{dx}{dt} = \lambda x + x^3$ (2.8)

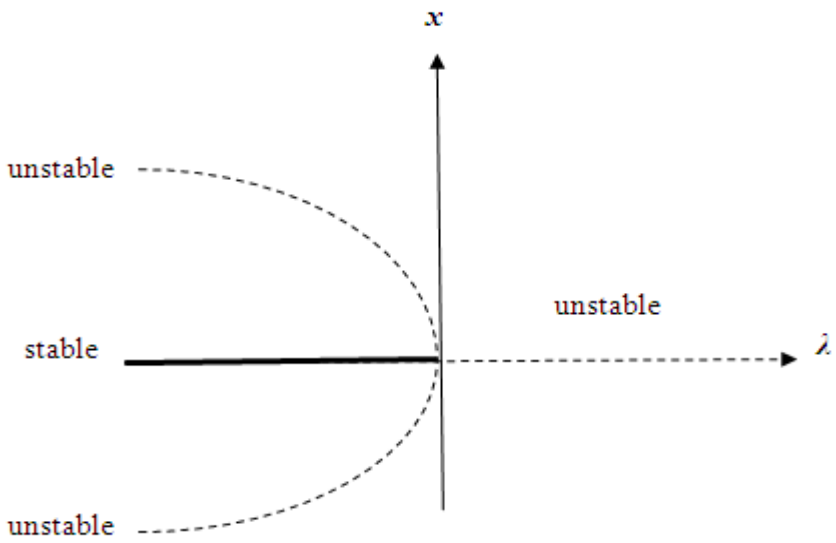

Figure 2.5: An example of subcritical pitchfork bifurcation.

Compared to Figure 2.4, the pitchfork is inverted. The nonzero steady state points $\pm\sqrt{-\lambda}$ are unstable and exist only below the bifurcation $(\lambda < 0)$, which motivates the term "subcritical". When $\lambda < 0$, the steady state at the origin is stable and suddenly becomes unstable when $\lambda > 0$.

Now, let us consider a more interesting subcritical pitchfork bifurcation.

Example: $\frac{dx}{dt} = \lambda x + x^3 + x^5$ (2.9)

To find the steady state points. Let the system equal to zero.

$$\frac{dx}{dt} = \lambda x + x^3 - x^5 = 0$$

$$\Rightarrow \quad x(\lambda + x^2 - x^4) = 0$$

$$\Rightarrow \quad \bar{x}_1 = 0 \tag{2.10}$$

$$\text{or} \quad \lambda + x^2 - x^4 = 0$$

$$x^2 = \frac{1 \pm \sqrt{1+4\lambda}}{2}$$

$$\bar{x}_{2,3} = \pm\left(\frac{1 \pm \sqrt{1+4\lambda}}{2}\right)^{1/2}; \lambda \geq -\frac{1}{4} \tag{2.11}$$

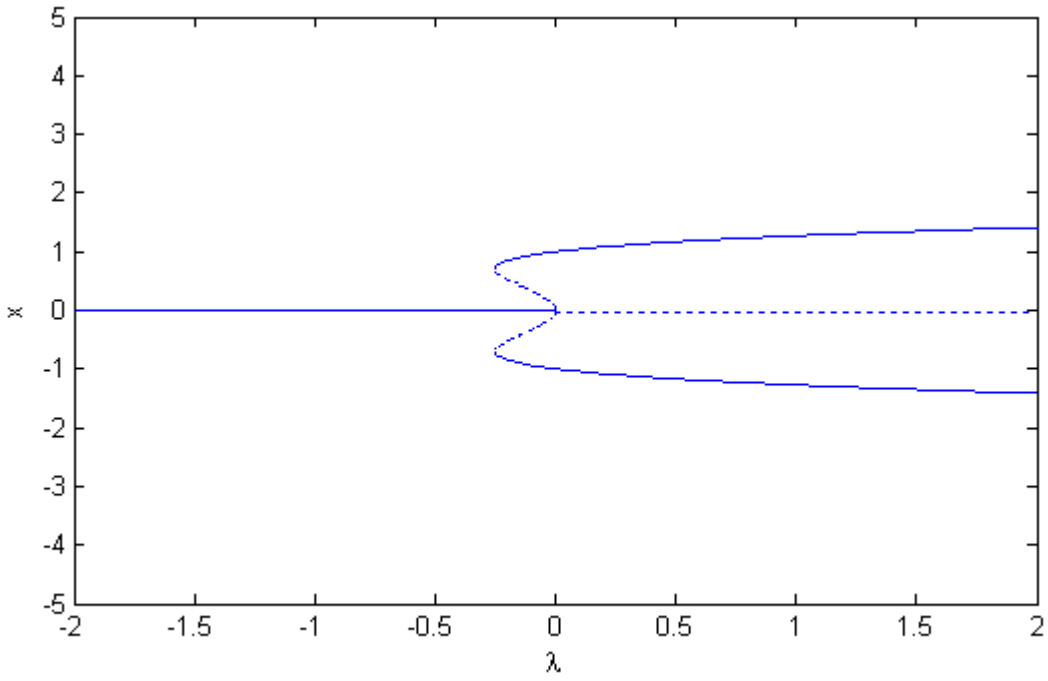

Figure 2.6: The bifurcation diagram for $\frac{dx}{dt} = \lambda x + x^3 - x^5$.

This bifurcation diagram (Figure 2.6) shows a lot of remarkable points to note. In the range of $\lambda_s < \lambda < 0$ (where $\lambda_s = -0.25$), two qualitatively different stable states coexist. The existence of different stable states allows for the possibility of *jumps* and *hysteresis* as λ is varied. Suppose that we start the system in the state $\bar{x}_1 = 0$, and then slowly we increase the value of λ. Then the state remains the stability until it reached $\lambda = 0$, the steady state $\bar{x}_1 = 0$ start losing its stability becomes unstable. Now, the slightest push of the value *x*, will cause the steady state to jump to one of the branches. As we increase λ, the steady state moves out along the large-amplitude branch. But if we decreased λ, the steady state stays at the large-amplitude branch, even if we decreased the value of λ below than 0. And if we lower the value of λ down past λ_S, only then the steady state jump back to $\bar{x}_1 = 0$. This lack of reversibility as a parameter is varied is call *hysteresis*. λ_S is the bifurcation point in which stable and unstable fixed points are born "out of the clear blue sky" as λ is increased. We can say that at point λ_S, it is a saddle-node bifurcation.

Hopf Bifurcation

Another bifurcation often encountered is the Hopf bifurcation. It arises when a spiral change its stability from stable to unstable and thus generates a branch of periodic solutions (i.e. limit cycles). The periodic solutions will have stability opposite to that of the spiral, but this will depend on which side of the bifurcation the periodic solutions are generated. There are two types of Hopf bifurcation. One in which stable limit cycles are created about an unstable steady state point called supercritical Hopf bifurcation. While, the other in which an unstable limit cycle is created about a stable steady state point, called the subcritical Hopf bifurcation.

2.1.4 Phase Portrait

A phase portrait is a geometric representation of the trajectories in a dynamical system in a phase plane. Each set of initial conditions is represented by a different curve or point.

Phase portraits are very useful tool in studying dynamical systems. They consist of a plot of typical trajectories in the state space. They reveal information such as whether an attractor, a repellor or limit cycle is present for the chosen parameter value. The concept of topological equivalence is important in classifying the behaviour of the systems by specifying when two different phase portraits represent the same qualitative dynamic behaviour.

A phase portrait of a dynamical system gives a picture of the system's trajectories, stable steady states and unstable steady states in a state space.

2.2 Example : Holling-Tanner Model

In this section, we will demonstrate those topics that we have covered previously. The Holling-Tanner Model has been studied both for its mathematical properties and its efficiency for describing real ecological systems such as mite / spider mite, lynx / hare, sparrow / sparrow hawk, etc.

Let us consider a specific Holling-Tanner Model (Braza, 2003) as the following:-

$$\begin{aligned}\frac{dx}{dt} &= x\left(1-\frac{x}{7}\right)-\left(\frac{6xy}{7+7x}\right)\\ \frac{dy}{dt} &= 0.2y\left(1-\frac{Ny}{x}\right)\end{aligned} \tag{2.12}$$

where N is a constant with $x(t)\neq 0$ and $y(t)$ representing the populations of prey and predator, respectively.

The term in the right-hand sides of the equations (2.12), have a physical meaning as follows:-

- The term $x\left(1-\frac{x}{7}\right)$ represents the usual logistic growth in the absence of predators.
- The term $-\frac{6xy}{7+7x}$ represents the effect of predators subject to a maximum predation rate.
- The term $0.2y\left(1-\frac{Ny}{x}\right)$ denotes the predator growth rate when a maximum of x/N predators is supported by x prey.

To construct a phase plane diagram, here are the steps that we need to take:-

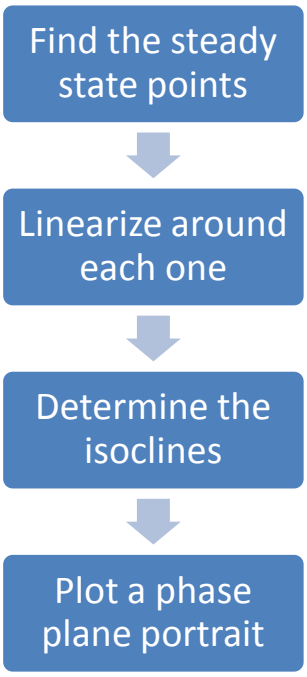

Suppose we want to sketch a phase portrait for this system when $N = 0.5$.

The steady state points are found by solving the equations $\frac{dx}{dt} = \frac{dy}{dt} = 0$.

$$\frac{dx}{dt} = x\left(1 - \frac{x}{7}\right) - \left(\frac{6xy}{7 + 7x}\right) = 0$$
$$\frac{dy}{dt} = 0.2y\left(1 - \frac{Ny}{x}\right) = 0 \qquad (2.13)$$

There are three steady state points in the first quadrant, namely, $A = (1,2)$, $B = (7,0)$,and this includes the origin. But we are only interested in steady states of *A* and *B*. Then, the Jacobian matrices are given by;

$$J_A = \begin{pmatrix} -1 & -\frac{3}{4} \\ 0 & \frac{1}{5} \end{pmatrix} \tag{2.14}$$

and

$$J_B = \begin{pmatrix} \frac{2}{7} & -\frac{3}{7} \\ \frac{2}{5} & -\frac{1}{5} \end{pmatrix} \tag{2.15}$$

The eigenvalues and eigenvectors of J_A are given by $\lambda_1 = -1, (1,0)^T$ and $\lambda_2 = \frac{1}{5}, \left(-\frac{5}{8}, 1\right)^T$. Therefore, this steady state point is a saddle point with stable manifold lying along the *x*-axis and the unstable manifold tangent to the line with slope $-\frac{8}{5}$ near to the steady state point. The eigenvalues of J_B are given by $\lambda \approx 0.043 \pm 0.335i$. Therefore, we can say that the steady state point at $B = (7,0)$ is an unstable spiral.

All trajectories lying in the first quadrant are drawn to the closed periodic cycle shown in the Figure 2.7 as the following:

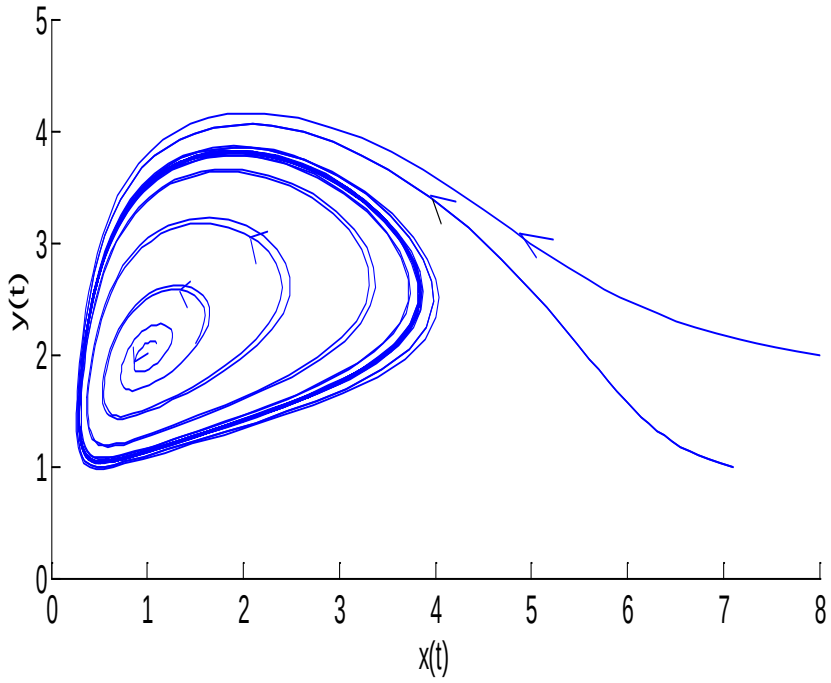

Figure 2.7: The phase plane diagram for Holling-Tanner Model where the trajectories are moving towards the limit cycle.

Therefore, no matter what the initial values of *x(t)* and *y(t)* are, the populations eventually rise and fall periodically. This isolated periodic trajectory is known as a limit cycle. In the long term, all trajectories in the first quadrant are drawn to this periodic cycle, and once there, will remain forever.

We try to do the same task but change the value of *N*. It shows that the system is structurally stable (or robust) since small perturbations do not affect the qualitative behaviour. The limit cycle will arise as a Hopf bifurcation on the steady states when *N* is a bifurcation parameter. To do this would require use of the path following method (XPPAUT) described in Chapter 5 which we do not do here. This predator-prey model oscillates in a similar manner to the Lotka-Volterra model with another major exception. The final steady state solution for the Holling-Tanner Model is independent of the initial conditions. This model appears to match very well with what happens for many predator-

prey species in the natural world – for example, house sparrows and sparrow hawks in Europe, muskrat and mink in Central North America, and white-tailed deer and wolf in Ontario.

CHAPTER 3

BIOLOGICAL BACKGROUND

In this chapter, we introduce a simple example on animal growth model that has been developed and some background of the previous models that being used in this project.

3.1 Simple Model for Animal Growth

Growth functions have an important role in animal nutrition partly, if not largely, because some growth functions are analytically soluble equations. Analytical models can be of great heuristic value. However, there are some quite simple models which do not permit analytical solutions, but are yet rather instructive and some of the simple models, the solutions are easy to obtain. Here is an example of a simple growth model as a dynamical system (Thornley and France, 2007).

'Open' Logistic Growth

The two-parameter logistic growth equation may be written:

$$\frac{dW}{dt} = \mu W\left(1 - \frac{W}{W_f}\right) \tag{3.1}$$

where: W : weight (state variable),

μ : a specific growth rate parameter,

W_f : final weight.

Given that $\mu = 0.2\,\text{day}^{-1}$, $W_f = 100\,\text{kg}$, $W(t=0) = W_0 = 1\,\text{kg}$.

The solution for (3.1) is

$$W(t) = \frac{W_0 W_f}{W_0 + (W_f - W_0)e^{-\mu t}} .$$

Growth is targeted on given final weight. For many animals, the final weight depends on conditions during the growth. It is easy to adjust parameter μ according to nutrition or temperature. However, this merely causes the animals to approach the final weight slower or faster. In the paper by Thornley and France (2005), they questioned the modification of W_f during growth according to actual growth conditions. Early limiting conditions produced a greater effect than late limitation. The degree of limitation is also important. A simple way to do the modification was proposed.

Equation (3.1) is replaced by two differential equations, with now three parameters:

$$\begin{aligned} \frac{dW}{dt} &= f_{\lim}\mu W\left(1 - \frac{W}{W_f}\right) \\ \frac{dW_f}{dt} &= -D(1 - f_{\lim})(W_f - W) \end{aligned} \tag{3.2}$$

W_f is now a state variable whose initial value assumes that there is no growth limitation. D is a development or differentiation rate. $f_{\lim}$ is a fraction, which reflects a possible growth limitation. The $\frac{dW_f}{dt}$ equation causes final weight W_f to move towards actual weight W at a rate depending on D times the degree to which growth is limited $(1 - f_{\lim})$. If $f_{\lim} = 1$, there is no growth limitation and W_f does not change from its initial value. If $f_{\lim} = 0$, there is no growth at all. Here, it is assumed, for simplicity, that the same growth-limiting factor $f_{\lim}$ occurs in the first and second of equation (3.2), affecting specific growth rate and change of asymptote.

While it is possible to eliminate W_f between these two differential equations and obtain a higher-order equation, this is not very helpful. Instead, we divide the two differential equations to eliminate dt and integrate (given constant parameters) to give:

$$\frac{W}{W_0} = \left(\frac{W_{f0}}{W_f} \right)^{\mu f_{\lim} / [D(1 - f_{\lim})]} \tag{3.3}$$

Here W_{f0} is the initial condition for W_f.

At the steady state, i.e. $t \to \infty$, W is equal to W_f. Let it be W_{max}.

$$\frac{W_f}{W_0} = \left(\frac{W_{f0}}{W_f} \right)^{\mu f_{\lim} / [D(1 - f_{\lim})]} \tag{3.4}$$

$$W_f^{\,1 + \frac{\mu f_{\lim}}{D(1 - f_{\lim})}} = W_0 W_{f0}^{\,\mu f_{\lim} / [D(1 - f_{\lim})]} \tag{3.5}$$

$$W_f = \left(W_0 W_{f0}^{\frac{\mu f_{\lim}}{D(1-f_{\lim})}} \right)^{\frac{1}{1+\frac{\mu f_{\lim}}{D(1-f_{\lim})}}} \tag{3.6}$$

$$W_{\max} = \left(W_0 W_{f0}^{\frac{\mu f_{\lim}}{D(1-f_{\lim})}} \right)^{\frac{1}{1+\frac{\mu f_{\lim}}{D(1-f_{\lim})}}} \tag{3.7}$$

Note that, with constant parameters, the asymptotic value of the animal weight depends on $\frac{\mu}{D}$.

Now, to illustrate the behaviour for the system (3.2), consider the following parameter values:

$\mu = 0.2\,\text{day}^{-1}$, $D = 0.1\,\text{day}^{-1}$, $0 \le f_{\lim} \le 1$,

$W(t=0) = W_0 = 1\,\text{kg}$, $W_f(t=0) = W_{f0} = 100\,\text{kg}$.

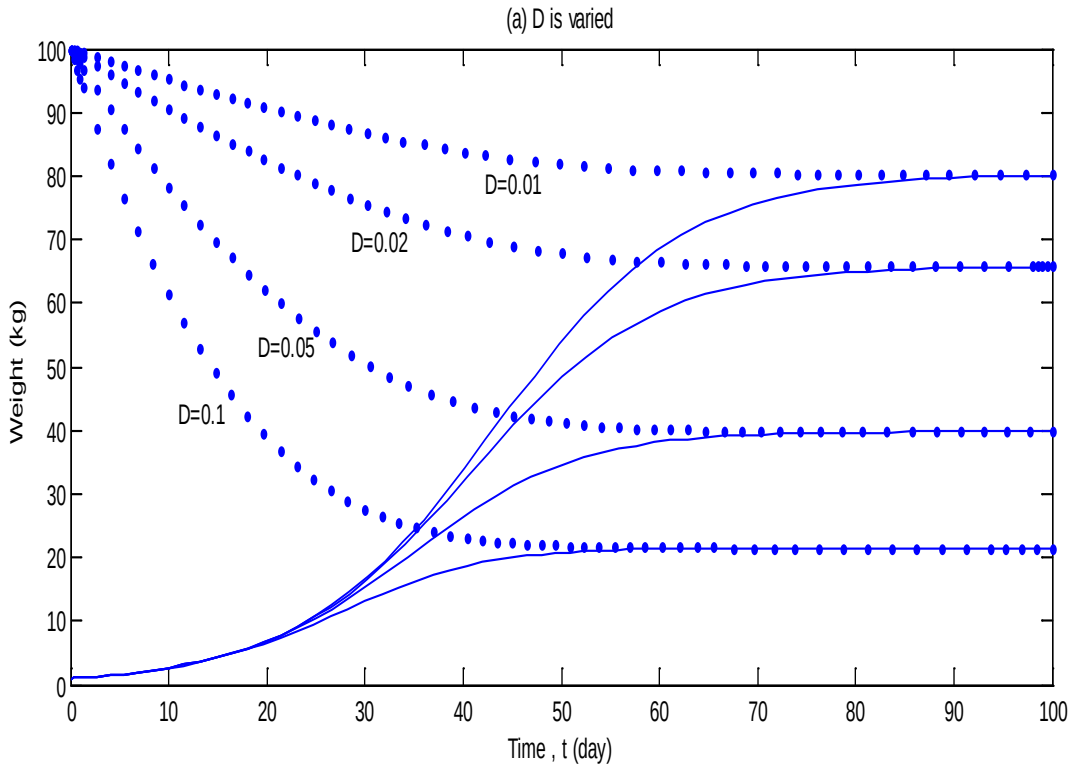

Figure 3.1: Solution of equation (3.2) with *D* is varied.

Figure 3.1 illustrates the behaviour of the open logistic equation when *D* is varied and the fixed value of $f_{\lim}$ at $f_{\lim} = 0.5$. Solid lines indicate weight, *W* and the dashed lines indicate the variable W_f. Both of which tend to the same asymptotic value. This figure shows that there is a change in final weight when we increased the value of *D*. This is due to the limitation, whereas if the development (*D*) is more comparable with growth (μ), then final weight can be much depressed.

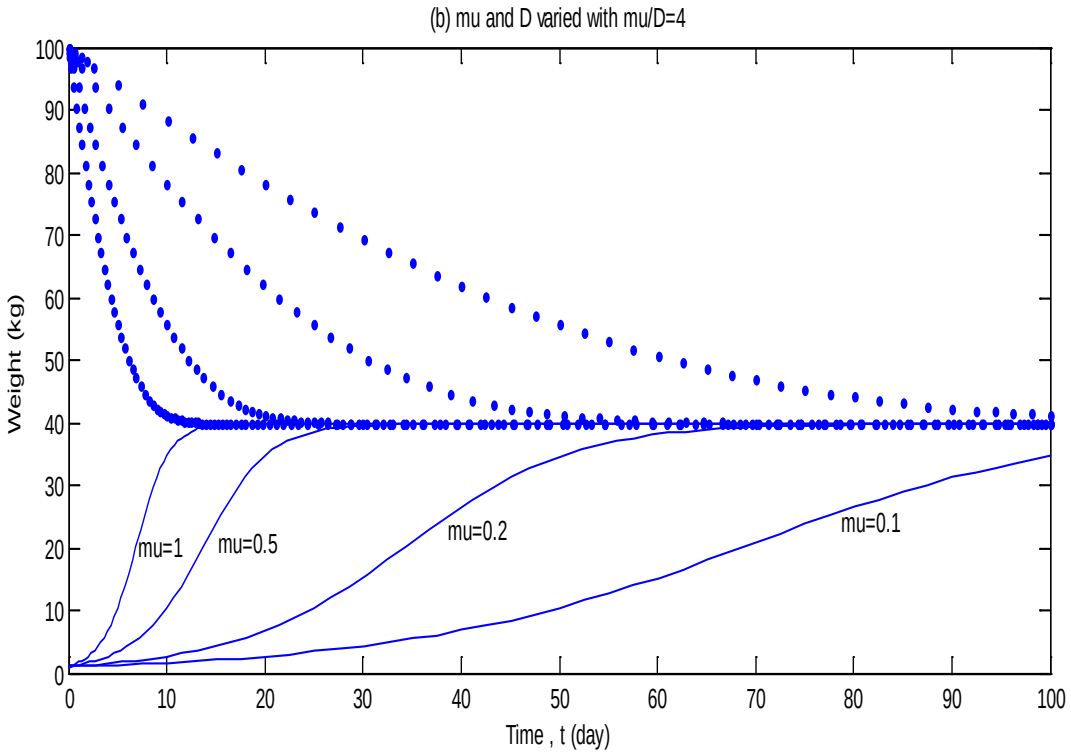

Figure 3.2: Solution of equation (3.2) with μ and *D* are varied.

Figure 3.2 illustrate the behaviour of the open logistic equation when μ and *D* are varied with $\frac{\mu}{D} = 4$. Solid lines indicate weight, *W* and the dashed lines indicate the variable W_f. It simply gives a picture of a changing timescale as we varying μ and *D* but maintaining the same ratio.

3.2 Review of Models in the Literature

For years, most studies in the field of animal nutrition have only focussed on the empirical models to developed animal growth models. It allows an animal's weight gain to be expressed as a relatively simple function and is often a curve-fitting exercise. However, it cannot give a real understanding of the system and may lack generality since it does not address the underlying mechanism. Numerous studies have attempted to explain the animal growth by mechanistic models (e.g. Oltjen and Sainz (1995); Freetly (1995)).

From the literature review, to more accurately predict growth on diets with extremes of energy, more complex models which can account for variable maintenance requirements or differing efficiencies of absorbed energy use are needed. To date, various methods have been developed and introduced to predict or measure the animal growth.

Vetharaniam *et al* (2001a, 2001b) have developed a mechanistic model of growth and pregnancy which is based on representation of a mammal, either for inclusion into a larger systems framework, or for modelling a single animal in its own right. In this study, they assume that the same principles of growth are used through fetal until post-natal stages and are similar among species. In spite of this, in dairy cows, not many studies have been done on the multiple protein pools in the animal growth model. But from current literature, there are few works done by Oltjen *et al* (2000, 2006) that described the multiple protein pools in the animal growth model. But Vetharaniam's paper might have been far more interesting if the authors had considered the body protein mobilization to accommodate changes in body composition specifically for dairy cows.

Furthermore, not many studies have been done on the mathematical analysis of the growth models and prediction of the response of an animal to various feeding strategies. In a Masters thesis by Wickham (1997), he investigated the construction and analysis of a number of models of animal growth, focusing on the protein pool and the interaction between muscular and visceral components. He also looked at how the behaviour of viscera and muscle were altered by changes in the model's parameters. Although, in the model by Vetharaniam *et al* (2001a, 2001b), the authors does mentioned on the growth rates at different feeding levels but they does not point out the behaviour of the dynamical system for different feeding level.

CHAPTER 4

A MODEL OF COMPOSITION AND GROWTH FOR MAMMALS

This chapter describes a model developed by Oliviera, Bywater and Vetharaniam (personal communication, July 2009) which was analysed in this project to identify the dynamical properties of the equations.

4.1 Model Description

This Masters thesis project investigates the model of Oliviera *et al* (personal communication, July 2009) to identify its stability and bifurcation structure. A model on a composition model of growth, pregnancy and lactation by Vetharaniam *et al* (2001a, 2001b), has been the basic foundation of the development of this model. The extension of the model is to accommodate the changes in body composition.

In most of the literature, they proposed the growth model as three compartments such as nutrient, fat and protein. But protein can be divided into two different types. One is slow turnover protein and the other one is fast turnover protein (viscera). From the model by Vetharaniam *et al* (2001a, 2001b), the animal laws were represented as two interacting pools, *N* (MJ), which is the energy available as a result of the energy flux through the blood and liver, plus free cellular energy and second, a pool of bound energy, *M* (kg), which identifies with the animal's empty body. Oliviera *et al* proposed that the animal be represented as four interacting pools. The tissue pool (*M*), will now be divided into lean body tissue or protein (*P*), viscera pool (*V*), and fat pool (*F*). This model attempts to describe the relationship between the protein, viscera and fat in growing farm animals, specifically dairy cows. A schema of the model is shown in Figure 4.1

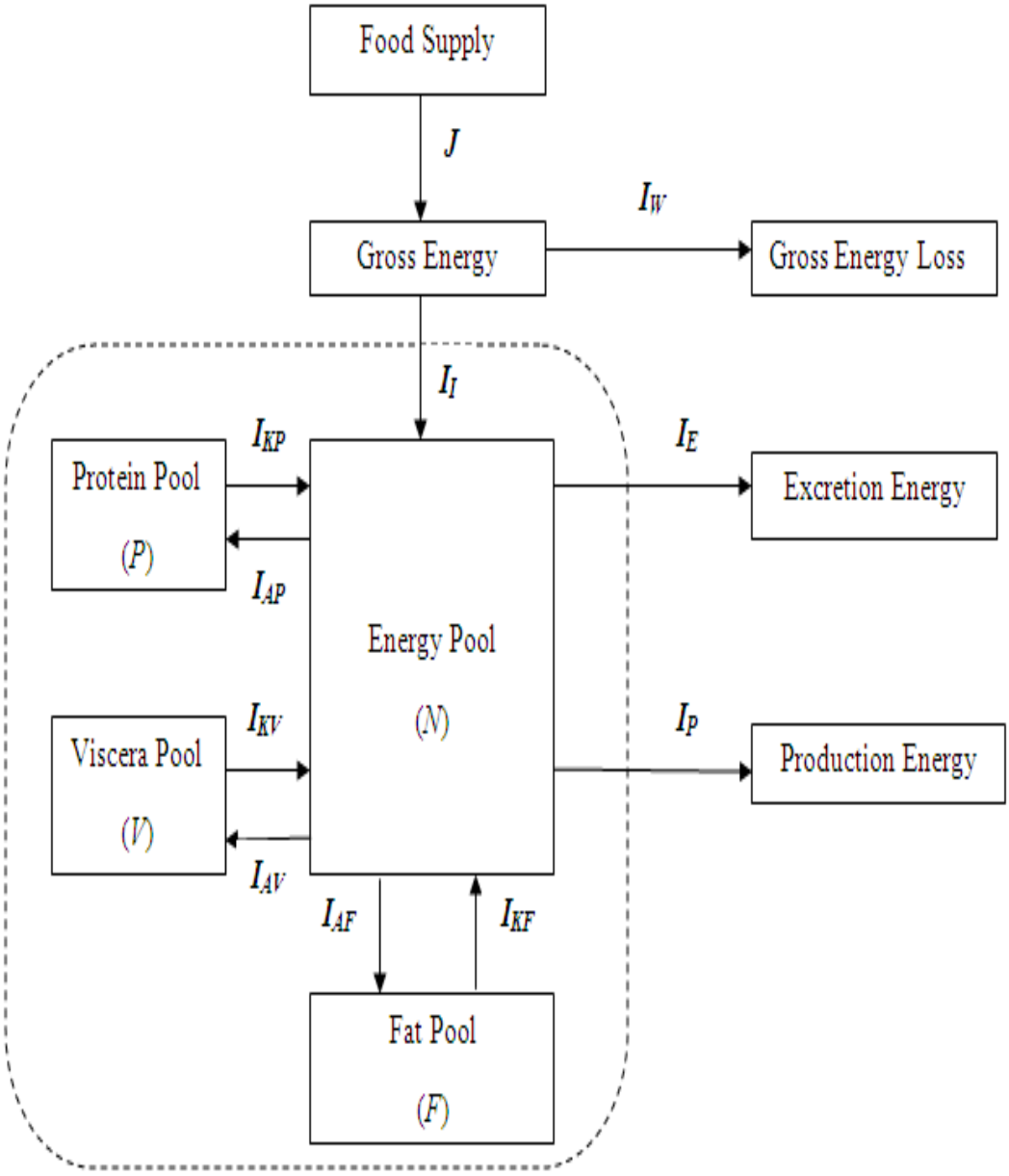

Figure 4.1: Model representation of animal's energetic (Oliviera *et al* model).

The animal eats and the food expressed as Gross Energy (GE) intake, J, is partitioned into Absorbed Energy (AE), I_I and wastes, I_W. Then, I_I flows into Energy Pool (N) and interacting with tissue pools such as protein (P), viscera (V) and fat (F). Anabolic currents flow from N to those tissue pools and provide the energy deposited as tissue in the tissue building process. At the same time, catabolic currents remove the energy from protein, viscera and fat pools back to N. Besides that, N also produced energy such as excretion energy (I_E) and production energy (I_P). Excretion energy, I_E, accounts for energy used for activity and to maintain body heat and for energy lost as urine. While production energy, I_P, accounts for energy used for lactation, conceptual supply and follicle growth.

The percentage of protein and fat in the body (and thus the energy content of the body) changes over time, and thus models of animal growth that represent the body as one pool need to take this into account when predicting growth. The model by Vetharaniam *et al* (2001a and 2001b) thus needed to evaluate the change in energy density over time in order to predict growth from a forage intake (specified in terms of energy consumed). This is not needed in the Oliviera *et al* model since the fat and protein pools are specified separately. The term $\frac{\partial \rho_M}{\partial t}$ (in Vetharaniam *et al* model) was there to accommodate a change in composition of the body as the animal matures. This is due to different water and ash content in the different pools. They also assumed the densities, ρ_P, ρ_V, ρ_F, to be constant over time. In this project, we are interested in the long-term behaviour of the system. For simplicity, we consider this animal growth model as an autonomous system since non-autonomous dynamical systems are much more difficult and complex to characterise than autonomous ones unless they have a particularly simple structure. Besides that, the model assumes the animal is not pregnant or lactating, and it does not expend energy to keep warm. Additionally, the energy cost of hair growth is ignored.

4.2 The Energy Dynamics

As in the paper by Vetharaniam *et al* (2001), the Absorbed Energy (AE) pool, *N*, acts as an intermediary for the flow of energy. The upper limit for *N*, *Nu*, is limited by the carrying capacity of the blood and intra cellular fluids. *Nu* is expressed in terms of free-energy with respect to protein, viscera and fat;

$$Nu = \rho_u \left(F + \frac{P+V}{c} \right) ; c = 0.23(\text{constant}) \tag{4.1}$$

where ρ_u [MJkg^{-1}] is the maximum energy pool density and is assumed constant.

If we refer to the previous figure on the animal's energetic (Figure 4.1), we can say that the dynamics of the absorbed energy pool, *N*, is the energy fluxes as:-

$$\frac{dN}{dt} = I_I + I_{K_P} + I_{K_V} + I_{K_F} - I_{A_P} - I_{A_V} - I_{A_F} - I_E \,. \tag{4.2}$$

where *N* [MJ] and *t* [days]. So, the units of the right-hand side functions are MJday^{-1}. I_I is the energy intake. I_{KP}, I_{KV}, I_{KF} are the catabolism currents and I_{AP}, I_{AV}, I_{AF} are the anabolism currents from protein, viscera and fat pools, respectively.

I_E is the excretion current (the energy needed to get rid of materials such as solid waste or urine from the body). This includes the heat from inefficiencies (I_ε) and the energy in urine (I_U) ;

$$I_E = I_\varepsilon + I_U . \tag{4.3}$$

Inefficiencies in tissue (I_ε) incur the anabolic energy (energy that causes muscle and bone growth) to be proportional to I_{AP}, I_{AV}, I_{AF} by $\varepsilon_{AP}, \varepsilon_{AV}, \varepsilon_{AF}$ respectively. At the same time, the heat from the catabolism (the process in an animal by which living tissue is changed into energy and waste products of a simpler chemical composition) is $\varepsilon_{KP} I_{KP}, \varepsilon_{KV} I_{KV}, \varepsilon_{KF} I_{KF}$ and the heat from the urea synthesis is $\varepsilon_U I_U$. All the ε factors are dimensionless.

So, we can say that the (I_ε) has a form as;

$$I_\varepsilon = \varepsilon_{A_P} I_{A_P} + \varepsilon_{A_V} I_{A_V} + \varepsilon_{A_F} I_{A_F} + \varepsilon_{K_P} I_{K_P} + \varepsilon_{K_V} I_{K_V} + \varepsilon_{K_F} I_{K_F} + \varepsilon_U I_U . \tag{4.4}$$

$\varepsilon_{AP}, \varepsilon_{AV}, \varepsilon_{AF}$ are the relative costs of anabolism due to protein, viscera and fat pool synthesis, respectively. $\varepsilon_{KP}, \varepsilon_{KV}, \varepsilon_{KF}$ are the relative costs of catabolism due to protein, viscera and fat pool degradation, respectively. ε_U is the urine synthesis.

Urinary energy is disintegrated into exogenous (external) and endogenous (internal) components. Exogenous urinary energy (from the deamination of dietary protein) is expressed as rI_I and the endogenous urinary energy are expressed as ηI_{KP} and ηI_{KV} ;

$$I_U = rI_I + \eta_P I_{K_P} + \eta_V I_{K_V} \tag{4.5}$$

here r is exogenous urine and r will vary with food source. While η_P, η_V are endogenous nitrogen excretion from protein and viscera, respectively. They are all dimensionless.

Metabolic Potentials for Protein, Viscera and Fat Pools

Each anabolic current from the protein, viscera and fat pools is associated with a "metabolic potential" or, the maximum rate of energy use, which is determined by degree of maturity and physiological state and a dimensionless "elasticity of supply" parameter which, together with N, govern the actual energy flow. Anabolic currents have a potential of Q_{AP}(protein), Q_{AV} (viscera) and Q_{AF} (fat). These have an elasticity of one and are met if $N = Nu$. The units of these potential currents are in MJday^{-1}.

So, I_{AP}, I_{AV} and I_{AF} have the form of:

$$I_{A_P} = \frac{N}{Nu} Q_{A_P} = \frac{N}{Nu}\left(w_{a_P} P\left(1 - \frac{P}{M_P}\right) + \frac{\kappa_P P}{1-\kappa_{A_P}}\right) , \quad (4.6)$$

$$I_{A_V} = \frac{N}{Nu} Q_{A_V} = \frac{N}{Nu}\left(w_{a_V} V\left(1 - \frac{V}{M_V}\right) + \frac{\kappa_V V}{1-\kappa_{A_V}}\right) , \quad (4.7)$$

$$I_{A_F} = \frac{N}{Nu} Q_{A_F} = \frac{N}{Nu}\left(w_{a_F} \frac{P}{M_P} F\left(1 - \frac{F}{M_F}\right) + \frac{\kappa_F F}{1-\kappa_{A_F}}\right) . \quad (4.8)$$

Note that in each anabolic current, there are logistic effects, where M_P, M_V and M_F are the carrying capacities. M_P, M_V, M_F [kg] are the maximum mass in protein, viscera and fat pools, respectively. w_{aP}, w_{aV}, w_{aF} [MJkg^{-1}day^{-1}] reflects the age dependence of anabolism. $\kappa_P, \kappa_V, \kappa_F$ [MJkg^{-1}day^{-1}] are the relative basal catabolism of protein, viscera and fat respectively and these terms are regard as constants. $\kappa_{AP}, \kappa_{AV}, \kappa_{AF}$ are the catabolism

related to anabolism of protein, viscera and fat respectively and they are dimensionless constants.

Catabolism Energy for Protein, Viscera and Fat Pools

There are three types of catabolism:-

1. Body turnover
2. Catabolism that associated with anabolism
3. Catabolism from the mobilisation of body tissue as an energy supply when the animal's absorbed energy (AE) intake is lower than its demand.

The rate of energy flow into *N* from the catabolism in the protein, viscera and fat pools are:-

$$I_{K_P} = \kappa_P P + \kappa_{A_P} I_{A_P} \tag{4.9}$$

$$I_{K_V} = \kappa_V V + \kappa_{A_V} I_{A_V} \tag{4.10}$$

$$I_{K_F} = \kappa_F F + \kappa_{A_F} I_{A_F} + \kappa_{N_F} F\left(1 - \frac{N}{Nu}\right)^7 \tag{4.11}$$

Schaefer and Krishnamurti (1984) indicate that I_{KP}, I_{KV}, I_{KF} are significant during active growth.

The first term in I_{KP}, I_{KV}, I_{KF} (i.e. $\kappa_P P, \kappa_V V, \kappa_F F$, respectively) are correspond to the body turnover since catabolism involved with body turnover can be expected to exhibit mass dependence.

The second terms $\kappa_{AP} I_{AP}, \kappa_{AV} I_{AV}, \kappa_{AF} I_{AF}$ are correspond to the catabolism that associated with anabolism. Oddy *et al* (1997) noted that degradation of protein increased with increased synthesis. It is assumed that constant $\kappa_{AP}, \kappa_{AV}, \kappa_{AF}$ of tissue being anabolised is then catabolised.

The term $\kappa_{NF} F\left(1-\frac{N}{Nu}\right)^7$ in I_{KF} is here because when an animal's supply of AE is lower than its demand, it must increase catabolism to maintain body processes and production demands. A decreased in AE will result in a lowering of the energy pool, *N*. The ratio of *N* to *Nu* is used as a replacement for the difference between energy demand and energy intake. κ_{NF} [MJkg^{-1}day^{-1}] is the catabolism due to energy deficit of fat pool. There is nothing particular significant about number seven in the exponent of the last logistic term. It is just to reflect the equivalence of turnover in each pool because the protein turnover will be more dominant than the turnover of body fat and to ensure that the term is significant only when *N* is much smaller than *Nu*.

Metabolic Potential for Energy Intake

The model specifies that the animal has an internal demand for absorbed energy of

$$Q_I = \frac{(1+\varepsilon_{A_P})Q_{A_P} + (1+\varepsilon_{A_V})Q_{A_V} + (1+\varepsilon_{A_F})Q_{A_F} - \kappa}{1 - r(1+\varepsilon_U)} \tag{4.12}$$

where ;

$$\kappa = [1-\varepsilon_{K_P} - \eta_P(1+\varepsilon_U)]I_{K_P} + [1-\varepsilon_{K_V} - \eta_V(1+\varepsilon_U)]I_{K_V} + (1-\varepsilon_{K_F})I_{K_F}$$

Q_I [MJday^{-1}] is the maximum absorbed energy intake of the animal will results in maximal rates for all its current flows. This means that the animal's energy demand, Q_I, is the sum of the metabolic potential for anabolism minus the catabolism energy from each of the protein, viscera and fat pools. We can say that Q_I is the metabolic potential for the energy intake I_I. Writing I_I as a fraction of Q_I is a convenient way to avoid modelling foraging and digestion.

$$I_I = \gamma Q_I \tag{4.13}$$

Here, γ is the driver for the feed intake. By letting $\gamma \in [0,1]$ indicate feeding level as ratio of the absorbed energy intake versus demand. In this project, we tried to analyse this animal growth model by controlling the value of γ.

κ is a catabolic offset of demand. κ is a "potential" which subtracts from the animal's energy demand because catabolism of tissue releases bound energy back into *N*, making it available for the animal's metabolic needs. Catabolism as an energy source can reduce the animal's need for energy from external sources. κ can be derived by requiring

$N = Nu$ which means let equation (4.2) equal to zero (i.e. $\frac{dN}{dt} = 0$) and substitute equation (4.3), (4.4) and (4.5) into this.

Growth

The rate of change of energy in the animal's empty body weight is the difference of the energy flows in minus the energy flows out.

$$\frac{dP}{dt} = \frac{1}{\rho_P}\left(I_{A_P} - I_{K_P}\right) \tag{4.14}$$

$$\frac{dV}{dt} = \frac{1}{\rho_V}\left(I_{A_V} - I_{K_V}\right) \tag{4.15}$$

$$\frac{dF}{dt} = \frac{1}{\rho_F}\left(I_{A_F} - I_{K_F}\right) \tag{4.16}$$

When the animal is at energetic static (the rate of the growth in each mass pools), we can say that anabolic current is equal to catabolic current.

i.e.

$$I_{AP} = I_{KP}$$
$$I_{AV} = I_{KV}$$
$$I_{AF} = I_{KF} \qquad (4.17)$$

since we know that $\rho_P, \rho_V, \rho_F \neq 0$.

CHAPTER 5

METHODOLOGY: XPPAUT APPROACH

In this chapter, we will provide a primer of the basic ideas and jargon of XPPAUT as a method of analysing the animal growth model.

5.1 Introduction

XPPAUT is a tool for simulating, animating and analysing dynamical systems. Most issues that we might want to do that related to dynamics either discrete or continuous can almost certainly be done with XPPAUT if we know how it works.

They are plenty of packages that will integrate differential equations. Software packages such as MATLAB, MAPLE and MATHEMATICA are recommended to study and analyse dynamical system. But these packages are slow when it comes to numerically solving differential equations and they do not offer much flexibility in the choice of integration methods and the integration is not done interactively. In XPPAUT, we can see

the progress of the solution until it is computed. Although MATLAB has great flexibility and can even integrate differential equations with discontinuities. However, the numerical integration is generally slower than can be achieved with XPPAUT. Moreover, the syntax of XPPAUT for setting differential equations is pretty simple compared to the other programs. What is more interesting about XPPAUT is that it is free and XPPAUT can be downloaded in the internet. In addition, in XPPAUT there are tools for analysing the system such as the plotting of Poincare sections, delayed embeddings, stability analysis, computation of one-dimensional invariant manifolds, nullclines and vector fields. Unlike the other software packages, they do not offer standard qualitative tools such as direction field and nullclines or they require additional packages or we need to write the code directly. XPPAUT also includes a frontend to AUTO, a continuation and bifurcation package. There is no packages offer an interface to AUTO. This self-contained version of AUTO communicates seamlessly with XPP making it easy to continue the solution to boundary value problems, as well as equilibria, fixed points and limit cycles.

5.2 How does XPPAUT work?

1. Creating ODE file

   To analyse a differential equations using XPPAUT, we must create an input file that tells the program the names of the variables, parameters and equations. By convention, these files have the file extension ode (abbreviation for ordinary differential equations).

   To create an ode file, these are the steps that should be taken:-

   1) Use an editor to open up a text line.
   2) Write the differential equations in the file; one per line.

3) Use the par statement to declare all the parameters in the system. We can define the initial conditions for the system with the `init` statement.
4) End the file with statement `done`.
5) Save the file with `filename.ode` and close the file.

XPPAUT is case sensitive. Therefore, one should not ever put spaces between the variables and the "=" sign and the number.

Every `.ode` file consists of declarations of the equations that we want to solve, the parameters involved and any user-defined functions that we will need. Note that in XPPAUT, the name of anything that is user-defined must be fewer than 10 characters.

2. Running the program

To run the program that we already saved, we need to start up XPPAUT with the filename (e.g. animalgrowth.ode). Then, a main window will appear which consists of a large region for graphics, menus and various other gadgets. To solve the ODE that we created, we just need to click on `InitialConds Go` in the main window. In XPPAUT, there are few numerical choices that we can choose to solve the ODE (such as Runge-Kutta, Stiff etc.). A solution will be drawn followed a beep. If we already computed a solution and we do not have any clue about the bounds of the graph, XPPAUT will resized it to a perfect fit by click on `Window/zoom Fit`. Not only that, we can just change the parameters and initial data values from the main window and we do not have to alter the program that we created in `.ode` file. In addition to the graphs that XPPAUT produces, it also gives us access to the actual numerical values from the simulation. Moreover, we can save the current state of XPPAUT that we are working on.

3. Quit the program

   To quit the program that we are running, it is easy. Just click `File Quit Yes` to exit XPPAUT.

5.3 Using AUTO: Bifurcation and Continuation

For many people, the main motive to use XPPAUT is because it provides a fairly simple interface to the continuation package, AUTO. AUTO has a graphical user interface in the distributed version, but still requires that we write in FORTRAN code to drive it. XPPAUT allows us to use most common feature of AUTO such as following fixed points, periodic orbits, homoclinic orbits and two-parameter continuations.

Many physical and biological systems include free parameters. One of the goals of applied mathematics is to understand how the behaviour of these systems varies as the parameters change. This is a numerically challenging task and there is generally no way to systematically explore a system as a function of all its parameters. What one should do is reduce the number of parameters either by fixing those which are best known or make the problem dimensionless. Assuming that we can reduce free parameters to a convenient number, there are some useful tools for exploring how a dynamical system changes as these parameters vary such as *continuation technique* (or also known as *path following technique*) in which a particular solution (such as a steady state point or limit cycle) is followed as the parameter changes. AUTO provides some very powerful algorithms for the continuation of steady state points and periodic solutions to differential equations. The

stability of the particular branch of solutions is readily obtained by analysing the linearization which is automatically accomplished by AUTO. If a steady state point or limit cycle exhibits a change in its stability, this is often a sign that new qualitatively different behaviour could occur. These qualitative changes in the local and global behaviour are called bifurcations and their detection during continuation is the subject of much mathematical research. AUTO provides a number of tools for the automatic detection of bifurcations of fixed points and limit cycles.

In the next section, we show how to use XPPAUT and AUTO together on a simple example of Morris-Lecar equations.

5.4 Illustration of XPPAUT

In this section, we are going to analyse an example of Morris-Lecar equations using XPPAUT. Morris-Lecar equations (Ermentrout, 2002) are a model for the membrane potential of a barnacle muscle, defined by the following equations:

$$\frac{dV}{dt} = I + g_l(E_l - V) + g_k w(E_k - V) + g_{c_a} m_\infty(V)(E_{c_a} - V)$$
$$\frac{dw}{dt} = (w_\infty(V) - w)\lambda_w(V) \qquad (5.1)$$

$$m_\infty(V) = 0.5\left(1+\tanh\left(\frac{V-V_1}{V_2}\right)\right)$$

where; $$w_\infty(V) = 0.5\left(1+\tanh\left(\frac{V-V_3}{V_4}\right)\right)$$

$$\lambda_w(V) = \phi\cosh\left(\frac{V-V_3}{2V_4}\right)$$.

Given that the parameter values as:

$I = 0$, $\phi = 0.333$,

$g_l = 0.5$, $g_k = 2$, $g_{c_a} = 1$,

$E_k = -0.7$, $E_{c_a} = 1$, $E_l = -0.5$,

$V_1 = -0.1$, $V_2 = 0.15$, $V_3 = 0.1$, $V_4 = 0.145$.

The variables are the membrane potential *V* and a gating variable *w* that represents activation of a potassium current. Let just assume that we are now referring to a dimensionless version of the Morris-Lecar equation and we will continue to do the analysis from here. In this example, we are trying to vary the value of current, *I* and the potassium current, ϕ. We want to analyse the behaviour of the system if we change the value of these parameters.

Firstly, we need to create the .ode file and let say we name it as morrislecar.ode. Then, start up XPPAUT and integrate this equation using `InitialConds` Go followed by `InitialConds` Last. By doing this, we are trying to tell XPPAUT to eliminate all the transients.

The solution and the phase plane for this system are (here *T* is time, *t*):

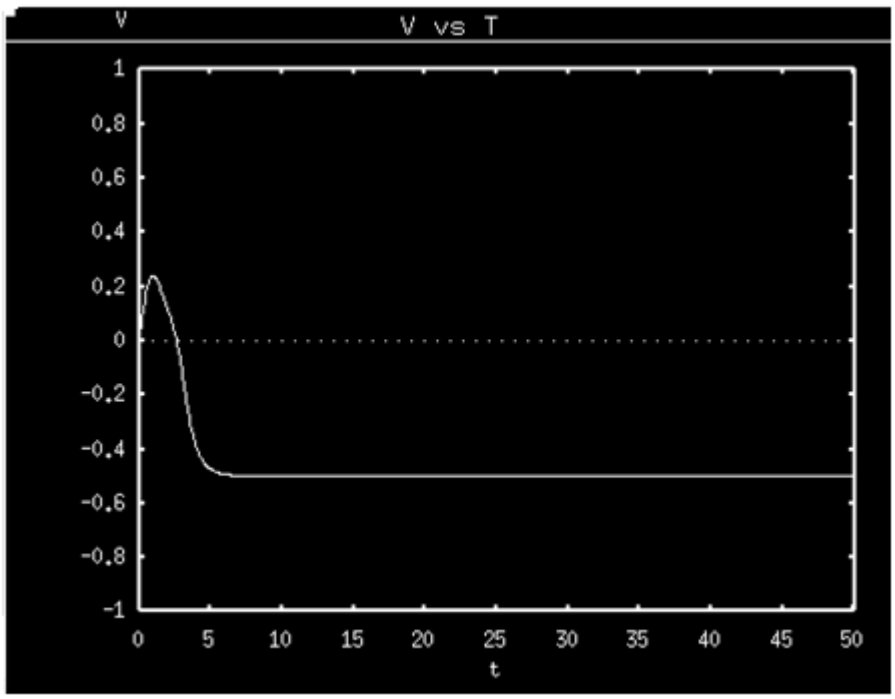

Figure 5.1: The solution graph for *V*.

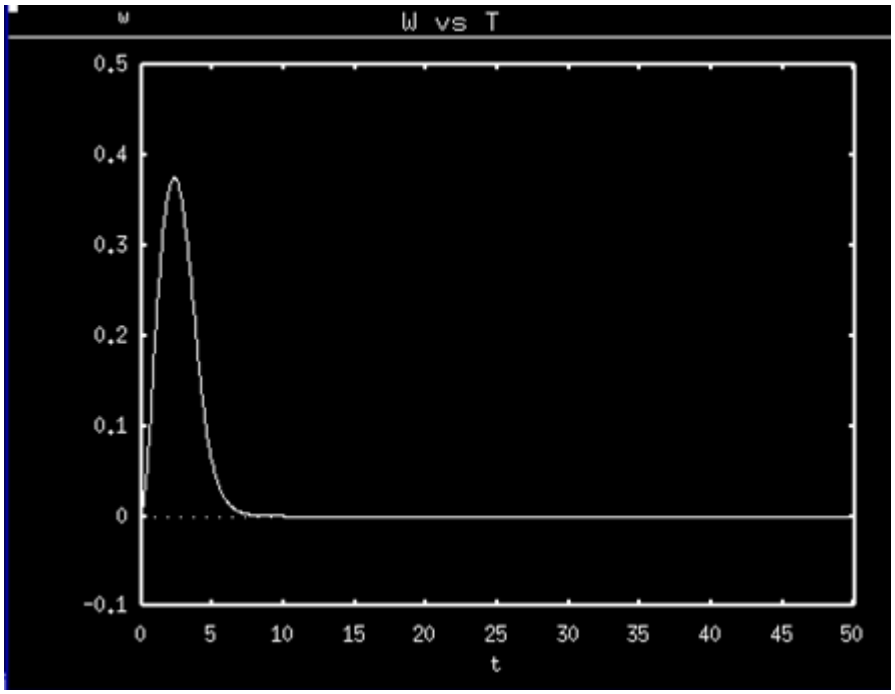

Figure 5.2: The solution graph for *w*.

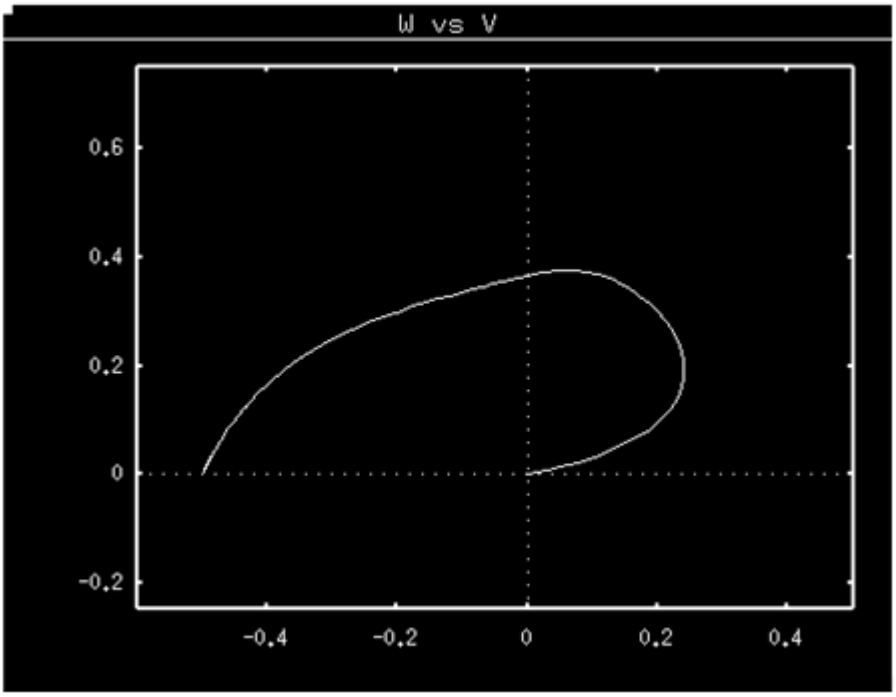

Figure 5.3: The phase plane diagram for Morris-Lecar equations, where *w* is plotted vertical and *V* on the horizontal with initial condition (0,0).

After that, click on `File Auto` to bring up AUTO. An AUTO window will appear as shown as below. From here on in, the rest of the commands will be in the AUTO window.

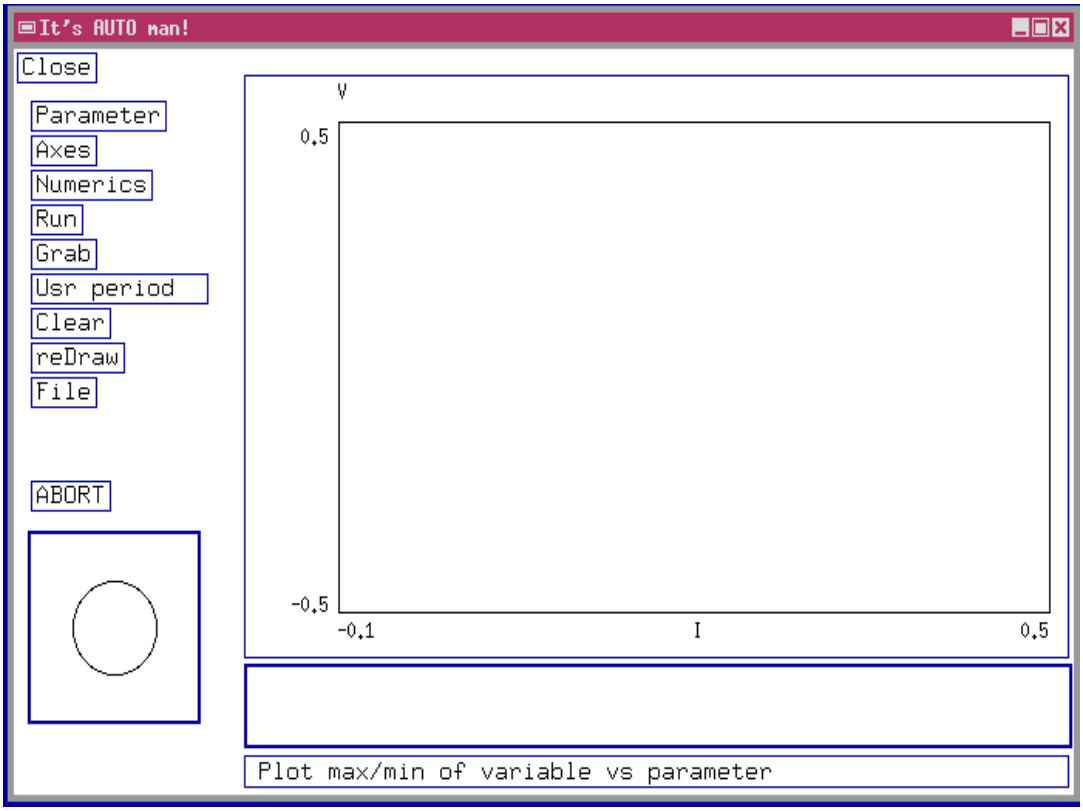

Figure 5.4: AUTO window in XPPAUT.

Click on `Axes Hi-Lo` to set up the graphics axes. We will set the axes as follows:-

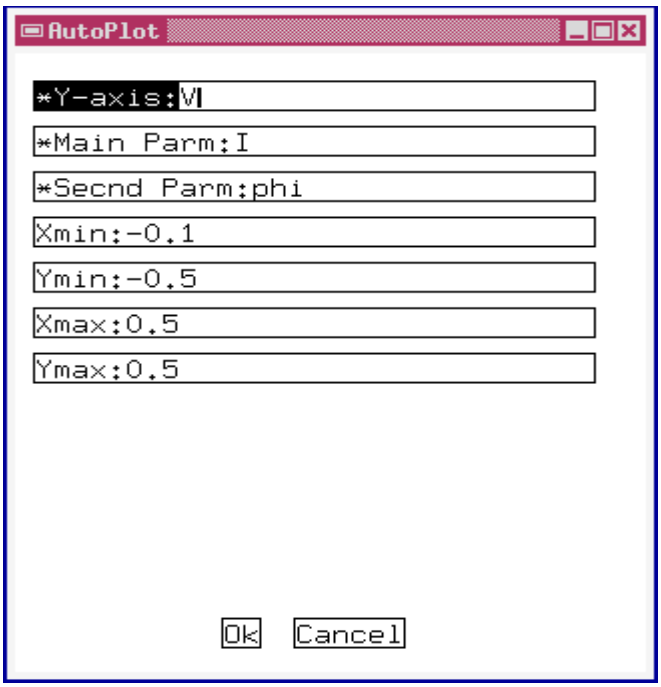

Next, click the `Numerics` and a dialog box will open. Change as follows:-

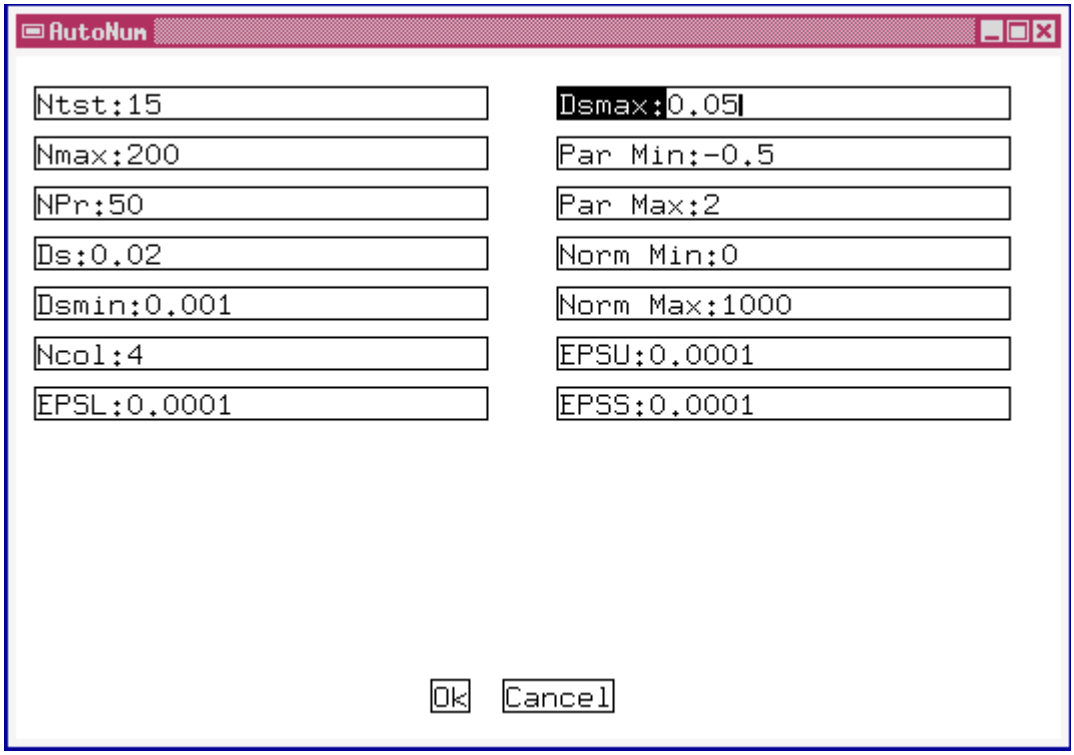

`Par Min` tells AUTO how far to continue the solution. While `Dsmax` set AUTO the maximum step to go to the direction of the solution. Then click `Ok`. To run the bifurcation, click on `Run Steady State`.

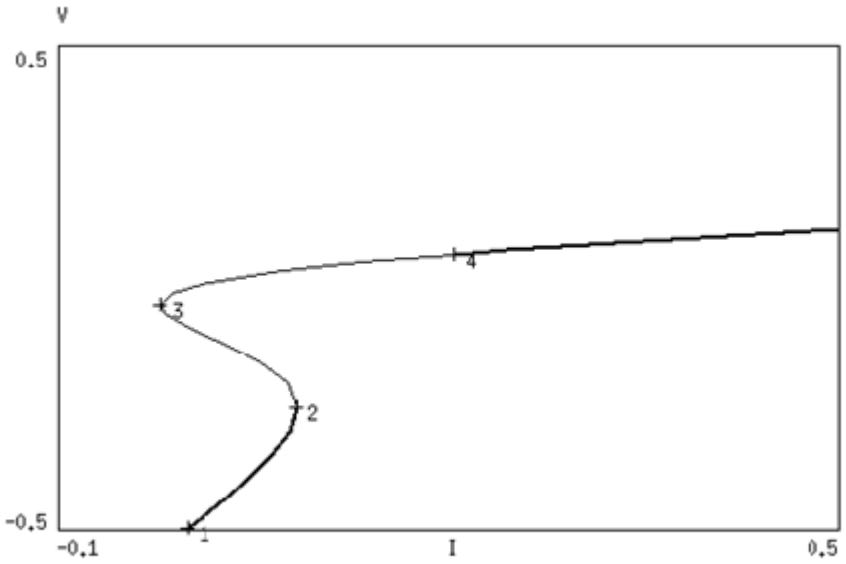

Figure 5.5: The bifurcation diagram with current, *I* is the parameter control. This diagram shows the stability of the steady state *V* as *I* is varied.

We should see a cubic curve with a few special points on it (see Figure 5.5) labelled as 1, 2, 3, 4 and 5 where the thick line corresponds to stable steady state and the thin line corresponds to unstable one. In this diagram, it shows that when the value of *I* is in the line between 1 and 2, the value of steady state *V* is stable. Whereas, as it reach point 2, it changed its stability (it becomes unstable). Again, it changes to be a stable steady state at point 4. Click on `Grab` and move through the diagram by tapping `Tab` on the keyboard. In the bottom of the AUTO window, there is a box shows the details of the points. One will see limit points (labelled LP) at $I = 0.08326$ and $I = -0.02072$ as well as an interesting Hopf bifurcation point (labelled HB) at $I = 0.20415$. We know that there is a periodic solution will occur at a Hopf bifurcation point. So, we press `Enter` at this point

(i.e. point 4) to grab it. By doing this, we try to compute the periodic orbit comes from this point. Click on `Run` and choose `Periodic`. One should see something as in Figure 5.6.

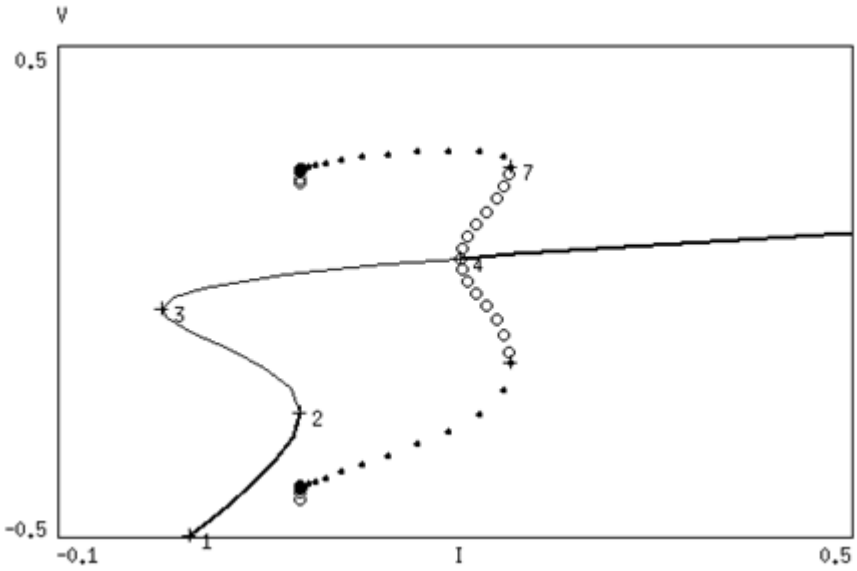

Figure 5.6: The Hopf bifurcation and the periodic solutions.

This diagram shows a number of interesting features that are quite important in bifurcation theory. Note that, the branch of periodic solutions that comes out of the Hopf point is unstable (open circles) and then it turns around at a limit point of oscillations at $I = 0.242$ (point labelled 7) where a stable and unstable limit cycle join together here. Therefore, if we perturbed a small range of currents, I (i.e. $I \in (0.15, 0.20415)$), there is a multiple stability between upper steady state and the limit cycle.

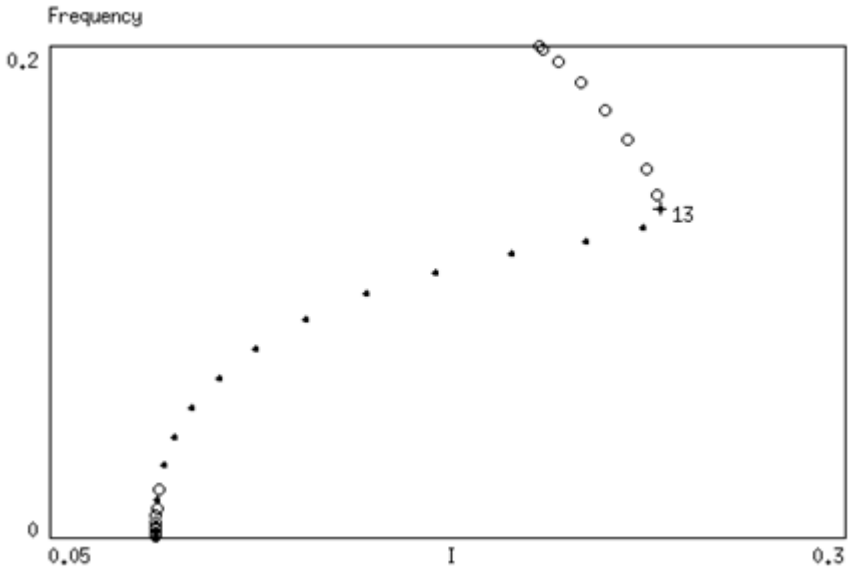

Figure 5.7: The frequency of the periodic solutions.

Now, let say we want to look at the two-parameter diagram for this model. Click on `Axes Two Par` and fill in the dialog box as below:

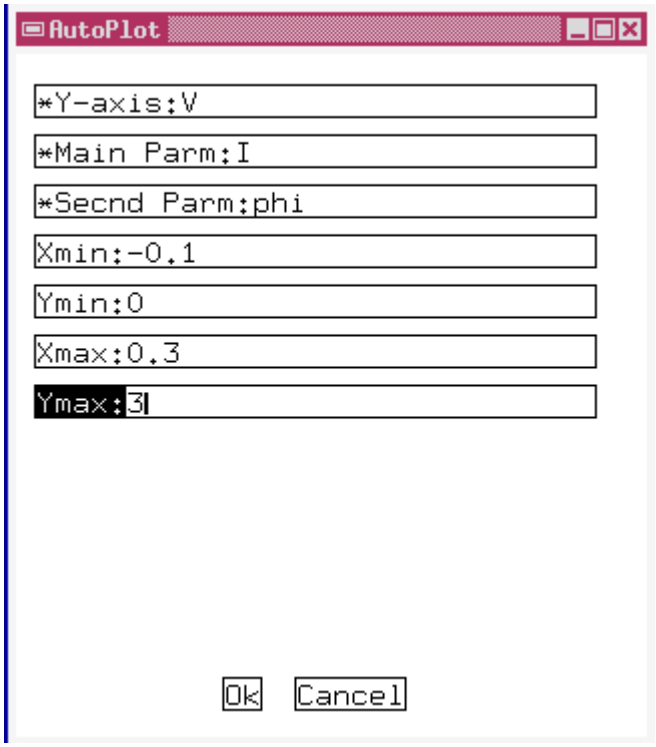

This will creates graph with I along x-axis and ϕ along y-axis. Click on `Grab` and press `Tab` key until reach the first limit point (LP) which should be labelled 2 and press `Enter` to grab it. Click on `Run`.

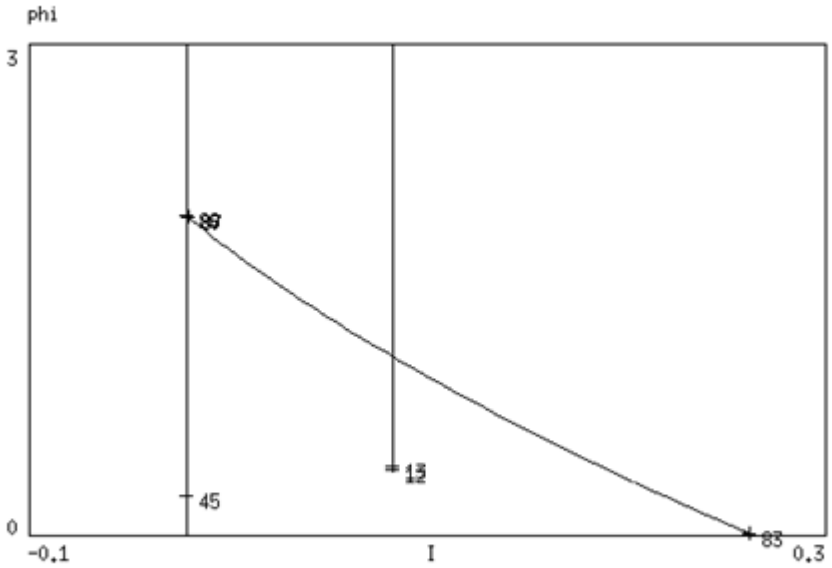

Figure 5.8: Two-parameter bifurcation diagram between I and ϕ.

A vertical line will appear (see Figure 5.8). This is because the limit point is independent of the parameter ϕ which has no effect on the value of steady state but can affect the stability of the system. Again click on `Grab` and `Tab` to the second limit point labelled 3. Click on `Run` and one should get another vertical line corresponding to the left most limit point. Next click on `Grab` and `Tab` to the Hopf bifurcation point (HB) labelled 4. Click on `Run Two Par` and one will see a curve going down and to the right. This is the curve of Hopf bifurcation points. Finally, we want to extend the curve of Hopf bifurcation points again. Click on `Numerics` and change `Ds` to `Ds=-0.02`. This means that we tell AUTO to go to the reverse direction. Finally, click on `Run Two Par`. One will see the curve go up and to the left. It crosses the right vertical line of folds points and stop at the left vertical line.

What we can tell from this diagram is that the right line represents the loss of the lower branch of the steady state. The termination of the curve of Hopf points on the left vertical line denotes a new higher-order bifurcation point.

For ϕ below the Hopf point curve and between the two vertical lines, the upper branch of steady state is unstable. On the right, it is stable above the Hopf curve and unstable below. On the left, the steady state is always stable. We can verify this by looking at the bifurcation diagram (Figure 5.6).

We will use this powerful tool to analyse the stability of the animal growth model (Oliviera *et al* model) in Chapter 6.

CHAPTER 6

ANALYSIS

In this chapter, we are about to illustrate the animal growth that have been developed by Oliviera *et al* and has been discussed in Chapter 4.

6.1 Analysis Part I

For this part, we try to do some analysis of the model proposed by Oliviera *et al* as we have been discussed in Chapter 4. At first, the animal growth model has a few numbers of free parameters. It is interesting to analyse how the behaviour of the system varies as the parameters change. This is a numerically difficult task to do the exploration of the system as a function of all its parameters. We did a sensible assessment of this animal growth model. We tried to reduce the free parameters to a convenient number. What we did was we take the system to be an autonomous system by ignoring the seasonal effects that were included by Oliviera *et al*, and by letting the time, t tend to infinity as we are interested in the long-term behaviour of the system. These seasonal effects are linked to day length and would cause the animal's mass to oscillate as it approached a maximum. Basically, what is

meant by that is, we only consider the growth of the animal in an aseasonal case. Aseasonal is an artificial situation where the animal experiences consistently long days and thus increased growth rates (Suttie and Webster, 1995; Tucker 1996).

Next, we try to run the model by setting different values of γ. It shows that something is missing here in the model because when $\gamma = 0.5$ (Figure 6.1(b)) and $\gamma = 0.75$ (Figure 6.1(c)), the growth for mass pools (*P*, *V*, *F*) and energy pool (*N*) of this animal tends to zero in less than 1000 days. When the model was developed, the biologist developing it did not have much data available and it only correspond to $\gamma = 1$ (Figure 6.1(a)). So, the parameterisation was not particularly robust as these results show (refer to Table 6.1).

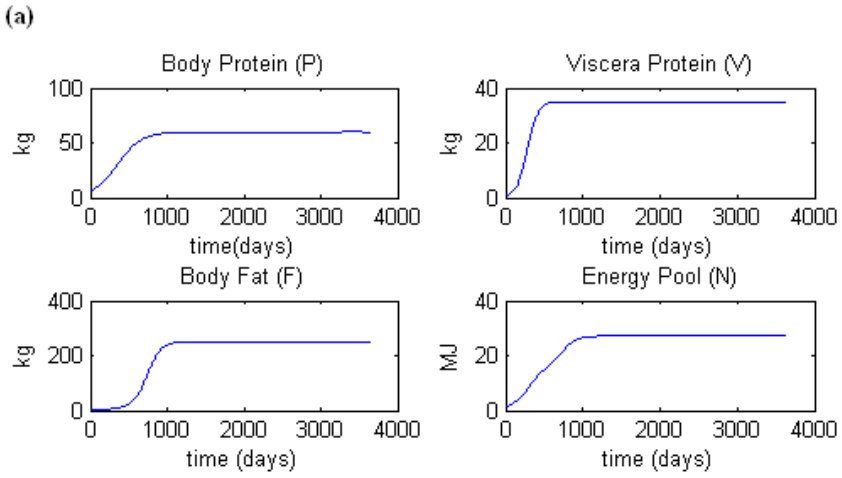

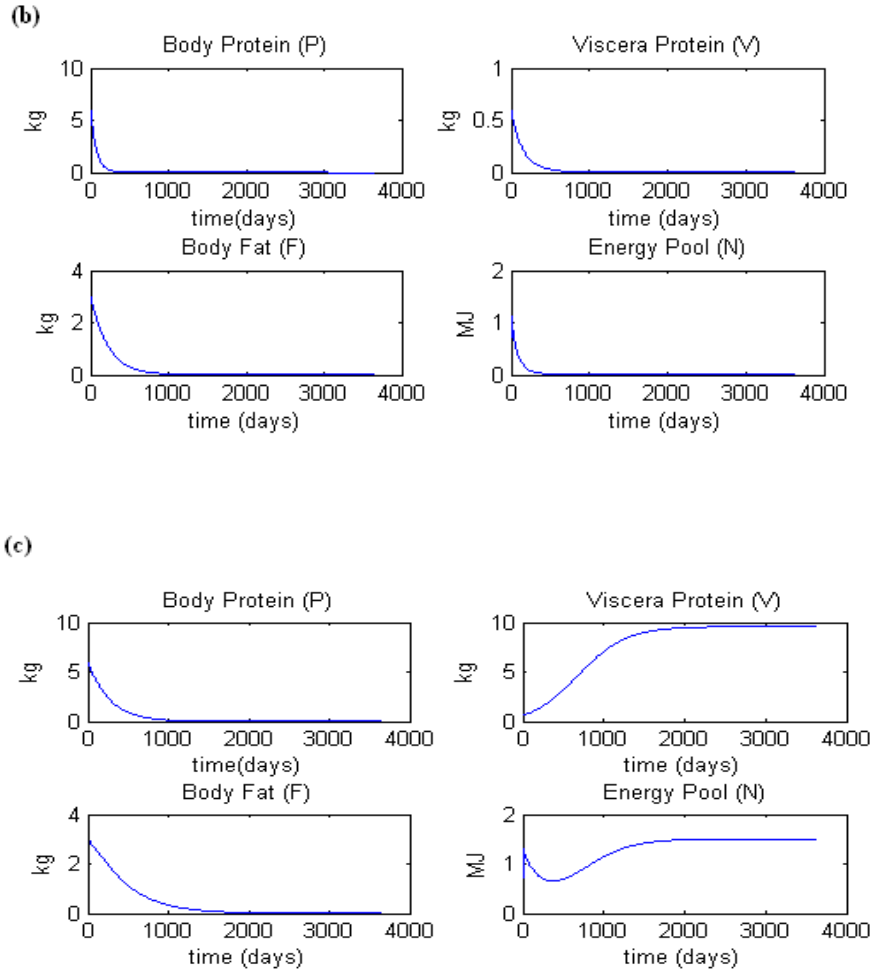

Figure 6.1: The graphs before parameterisation. (a) correspond to $\gamma = 1$, (b) correspond to $\gamma = 0.5$ and (c) correspond to $\gamma = 0.75$.

Symbol	Description	Value	Units
ρ_u	Maximum energy pool density	0.04100	$MJkg^{-1}$
ε_{A_p}	Relative cost of anabolism due to protein synthesis	0.25000	
ε_{A_V}	Relative cost of anabolism due to viscera synthesis	0.25000	

ε_{A_F}	Relative cost of anabolism due to fat synthesis	0.33000	
ε_{K_P}	Relative cost of catabolism due to protein degradation	0.20000	
ε_{K_V}	Relative cost of catabolism due to viscera degradation	0.20000	
ε_{K_F}	Relative cost of catabolism due to fat degradation	0.15000	
ε_U	Urine synthesis	0.35000	
η_P	Endogenous nitrogen excretion from protein pool	0.04200	
η_V	Endogenous nitrogen excretion from viscera pool	0.04200	
r	Exogenous urine (AE)	0.07800	
ρ_P	Protein density pool	23.1000	$MJkg^{-1}$
ρ_V	Viscera density pool of protein, viscera (protein +fat) and fat	23.1000	$MJkg^{-1}$
ρ_F	Fat density pool	38.5000	$MJkg^{-1}$
κ_P	Relative basal catabolism of protein	1.80000	$MJkg^{-1}day^{-1}$
κ_V	Relative basal catabolism of viscera	1.80000	$MJkg^{-1}day^{-1}$
κ_F	Relative basal catabolism of fat	0.80000	$MJkg^{-1}day^{-1}$
κ_{A_P}	Catabolism related to anabolism of protein pool	0.15000	
κ_{A_V}	Catabolism related to anabolism of viscera pool	0.55384	

κ_{A_F}	Catabolism related to anabolism of fat pool	0.10000	
κ_{N_F}	Catabolism due to energy deficit of fat pool	0.03180	$MJkg^{-1}day^{-1}$
w_{a_p}	Parameter that related to growth in protein pool	0.17000	$MJkg^{-1}day^{-1}$
w_{a_v}	Parameter that related to growth in viscera pool	0.75000	$MJkg^{-1}day^{-1}$
w_{a_F}	Parameter that related to growth in fat pool	1.45000	$MJkg^{-1}day^{-1}$
M_P	Maximum mass in protein pool	55	kg
M_V	Maximum mass in viscera pool	30	kg
M_F	Maximum mass in fat pool	250	kg

Table 6.1: The values for the parameters in the model determined from data.

So, we did re-parameterised the model and change one of the equations. Firstly, we change the equation (4.8).

From this,

$$I_{A_F} = \frac{N}{Nu} Q_{A_F} = \frac{N}{Nu}\left(w_{a_F} \frac{P}{M_P} F\left(1-\frac{F}{M_F}\right) + \frac{\kappa_F F}{1-\kappa_{A_F}} \right)$$

to this form,

$$I_{A_F} = \frac{N}{Nu} Q_{A_F} = \frac{N}{Nu}\left(w_{a_F} F\left(1 - \frac{F}{M_F \dfrac{P}{M_P}}\right) + \frac{\kappa_F F}{1-\kappa_{A_F}}\right). \qquad (6.1)$$

Here, we have re-examined the physiological formulation of the equation to better reflect the physical relationships in the model. Specifically, we changed the effectively "carrying capacity" in the logistic term to include the changing ratio $\frac{P}{M_P}$.

The next thing we did was changed some of the parameter values so that the model is realistic when the value of γ is decreasing (see Table 6.2).

Symbol	Description	Value	Units
ρ_u	Maximum energy pool density	0.04100	$MJkg^{-1}$
ε_{A_P}	Relative cost of anabolism due to protein synthesis	0.25000	
ε_{A_V}	Relative cost of anabolism due to viscera synthesis	0.25000	
ε_{A_F}	Relative cost of anabolism due to fat synthesis	0.33000	
ε_{K_P}	Relative cost of catabolism due to protein degradation	0.20000	
ε_{K_V}	Relative cost of catabolism due to viscera degradation	0.20000	
ε_{K_F}	Relative cost of catabolism due to fat degradation	0.15000	

ε_U	Urine synthesis	0.35000	
η_P	Endogenous nitrogen excretion from protein pool	0.04200	
η_V	Endogenous nitrogen excretion from viscera pool	0.04200	
r	Exogenous urine (AE)	0.07800	
ρ_P	Protein density pool	23.1000	$MJkg^{-1}$
ρ_V	Viscera density pool of protein, viscera (protein +fat) and fat	23.1000	$MJkg^{-1}$
ρ_F	Fat density pool	38.5000	$MJkg^{-1}$
κ_P	Relative basal catabolism of protein	0.50000	$MJkg^{-1}day^{-1}$
κ_V	Relative basal catabolism of viscera	0.50000	$MJkg^{-1}day^{-1}$
κ_F	Relative basal catabolism of fat	0.20000	$MJkg^{-1}day^{-1}$
$\mathcal{K}_{A_P}$	Catabolism related to anabolism of protein pool	0.10000	
$\mathcal{K}_{A_V}$	Catabolism related to anabolism of viscera pool	0.35000	
$\mathcal{K}_{A_F}$	Catabolism related to anabolism of fat pool	0.03000	
$\mathcal{K}_{N_F}$	Catabolism due to energy deficit of fat pool	0.03180	$MJkg^{-1}day^{-1}$
w_{a_p}	Parameter that related to growth in protein pool	0.50000	$MJkg^{-1}day^{-1}$
w_{a_v}	Parameter that related to growth in viscera pool	1.00000	$MJkg^{-1}day^{-1}$

w_{a_F}	Parameter that related to growth in fat pool	2.00000	$MJkg^{-1}day^{-1}$
M_P	Maximum mass in protein pool	55	kg
M_V	Maximum mass in viscera pool	30	kg
M_F	Maximum mass in fat pool	250	kg

Table 2: The values of the parameters after parameterisation.

6. 2 Analysis Part II

6.2.1 Solution Graphs

So, the animal growth model is simply a set of autonomous ODEs. Recall that the equations are;

$$\begin{aligned}
\frac{dN}{dt} &= I_I + I_{KP} + I_{KV} + I_{KF} - I_{AP} - I_{AV} - I_{AF} - I_E \\
\frac{dP}{dt} &= \frac{1}{\rho_P}(I_{AP} - I_{KP}) \\
\frac{dV}{dt} &= \frac{1}{\rho_V}(I_{AV} - I_{KV}) \\
\frac{dF}{dt} &= \frac{1}{\rho_F}(I_{AF} - I_{KF})
\end{aligned} \quad . \qquad (6.1)$$

This animal growth model equation is amenable to solution by a variety of methods. Since the system is stiff, all integration is done by using Stiff Method. Some of the values of the

parameters for this model were taken from other authors' experimental work which was given in Table 6.2.

The values for these parameters are to be seen as a starting point for an exploration of the surrounding parameter space rather than a fixed set of values. As mentioned in the previously chapter, we are interested in how this animal growth system behave when we try to vary the value of the feeding level, γ.

Here, we tried to find the solution graphs for nutrient (N), protein (P), viscera (V) and fat (F). We set the initial values as:-

$$P(0) = 6\,; \qquad V(0) = 0.6\,; \qquad F(0) = 3$$

And the initial value of N is given as;

$$N(0) = 0.5 \times \rho_u \times \left(F(0) + \frac{P(0) + V(0)}{0.23} \right). \tag{6.2}$$

In particular, we consider for various values of feeding level to determine the steady state and plot the trajectories.

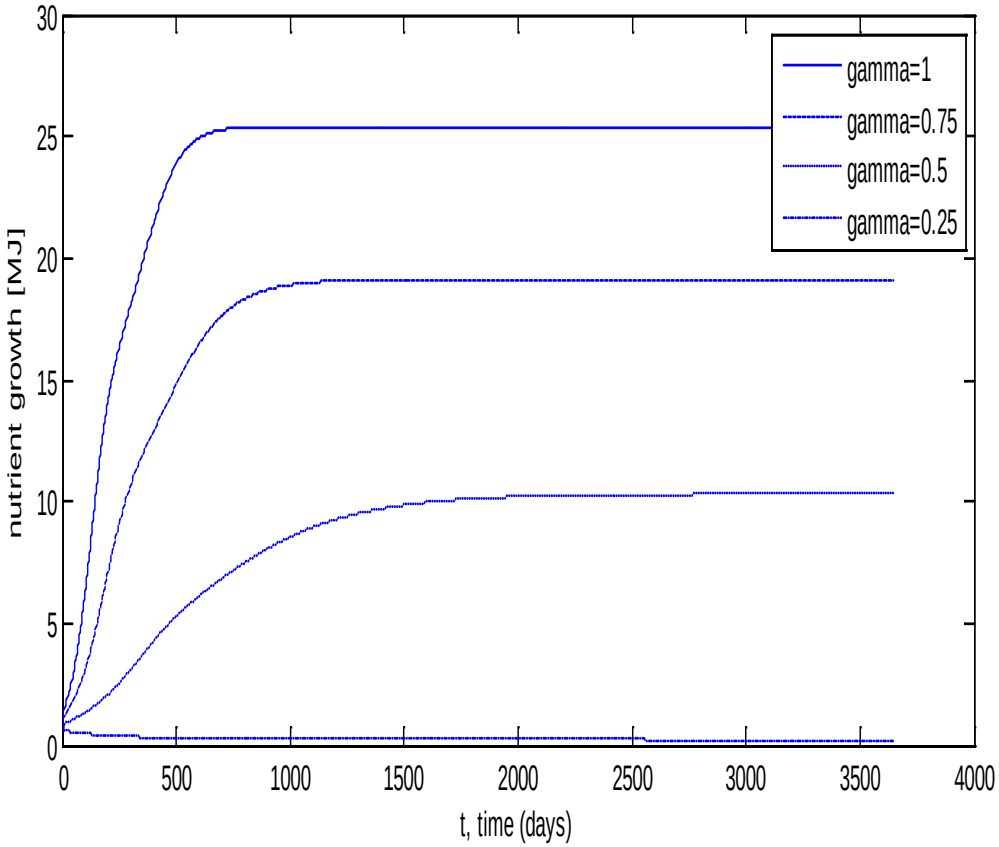

Figure 6.2: Solution graph for nutrient (N) at the different values of γ.

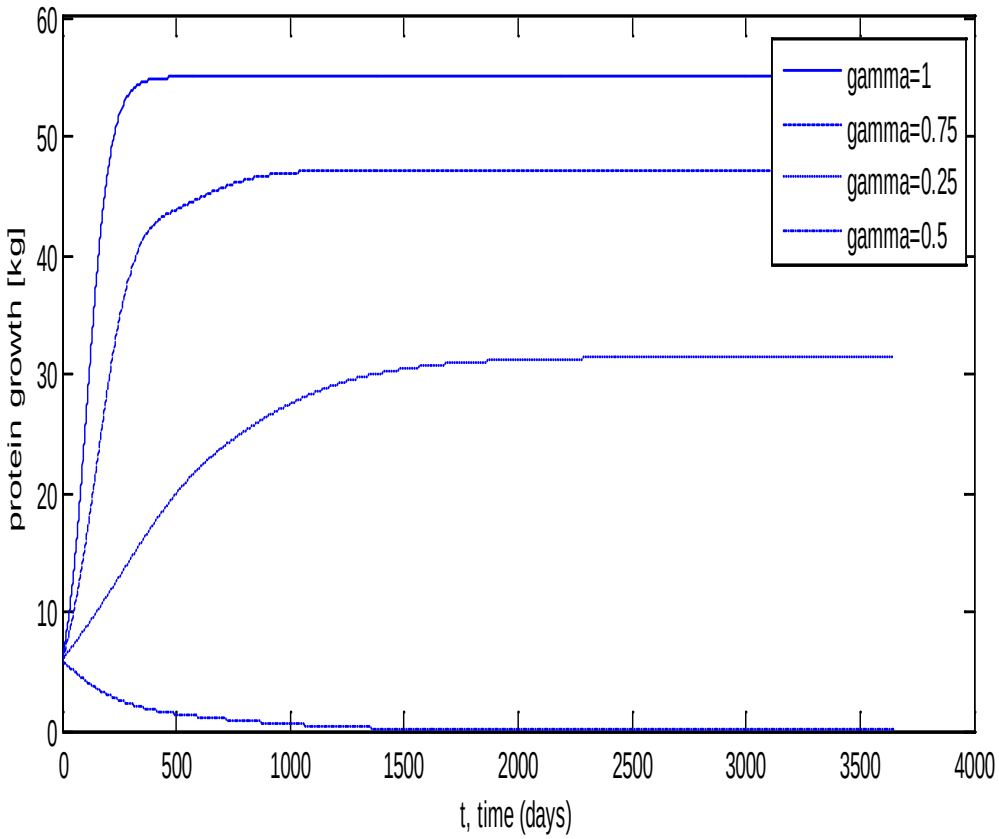

Figure 6.3: Solution graph for protein (P) at the different values of γ.

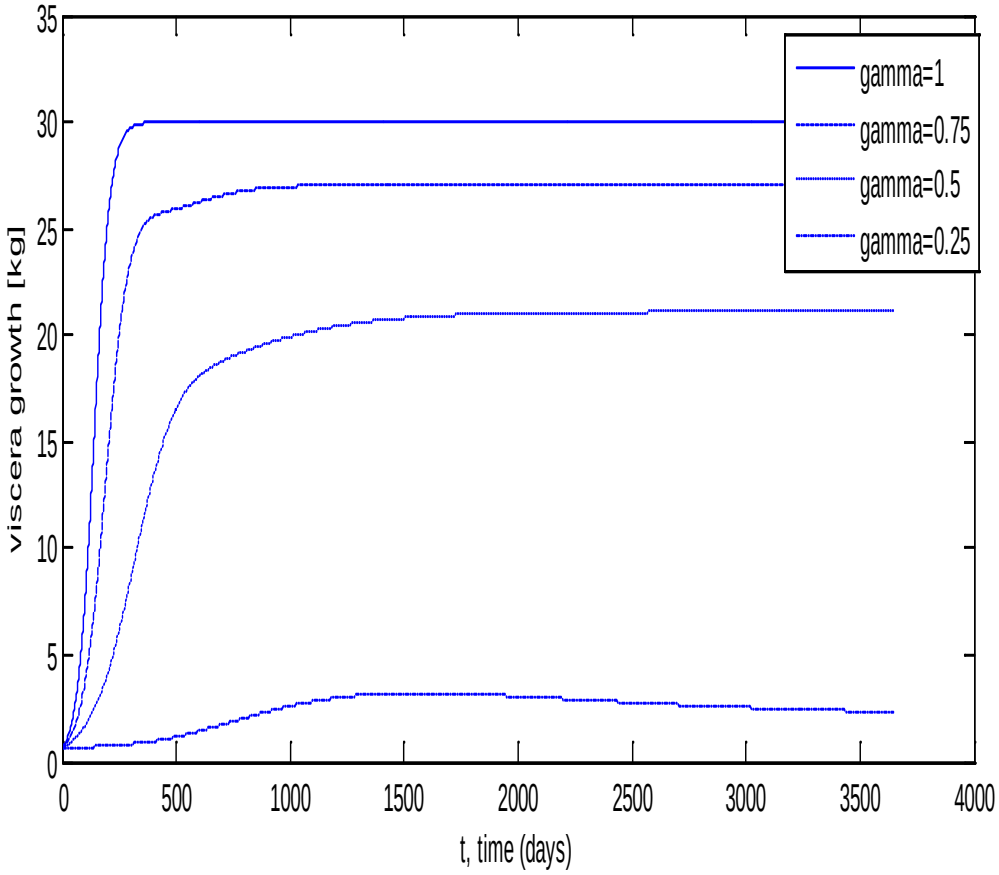

Figure 6.4: Solution graph for viscera (V) at the different values of γ.

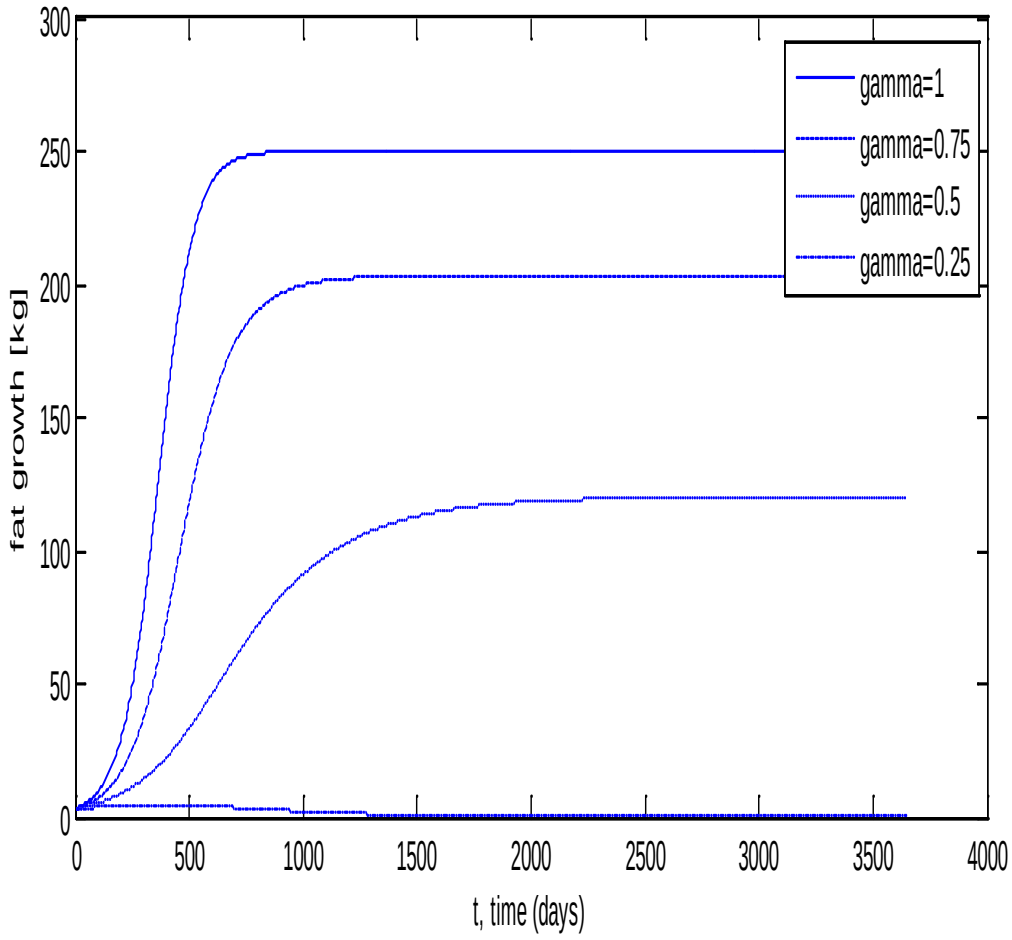

Figure 6.5: Solution graph for fat (F) at the different values of γ.

Figures (6.2, 6.3, 6.4 and 6.5) show the results of integrating the system with respect to time until 3650 days. It shows the growth of an animal for nutrient (*N*), protein (*P*), viscera (*V*) and fat (*F*) pools with a number of different feeding levels. When $\gamma = 1$, it corresponds to the maximal feeding ($I_I = \gamma Q_I$). But when $\gamma = 0.75, \gamma = 0.5, \gamma = 0.25$, they correspond to intakes of 75%, 50% and 25% of maximal feeding, respectively. It means that the animal is limited by its potential to utilise energy. The growth is from birth to maturity of an animal with no exercise or production requirements.

From the figures, in general, it shows that the graphs are to increase for a certain amount of time before it reaches a steady state. The model predicts that nutrient, protein, viscera and fat in the animal are at its highest when $\gamma = 1$ and it decreases as the value of γ decreases. Moreover, note that when γ is very small (let us consider $\gamma = 0.25$), the energy and the mass pools did not increase all but decreases as animal tends to maturity. In other words, the animal is dying. Besides that, the model predicts the higher value of γ, the faster the system reaches the steady state as can be seen on the graphs. Not only that, for a higher level of γ, the smaller change in the steady state between levels. The difference between the amount of nutrient and the mass pools when $\gamma = 1$ and when $\gamma = 0.75$ is smaller than the difference between $\gamma = 0.75$ and $\gamma = 0.5$.

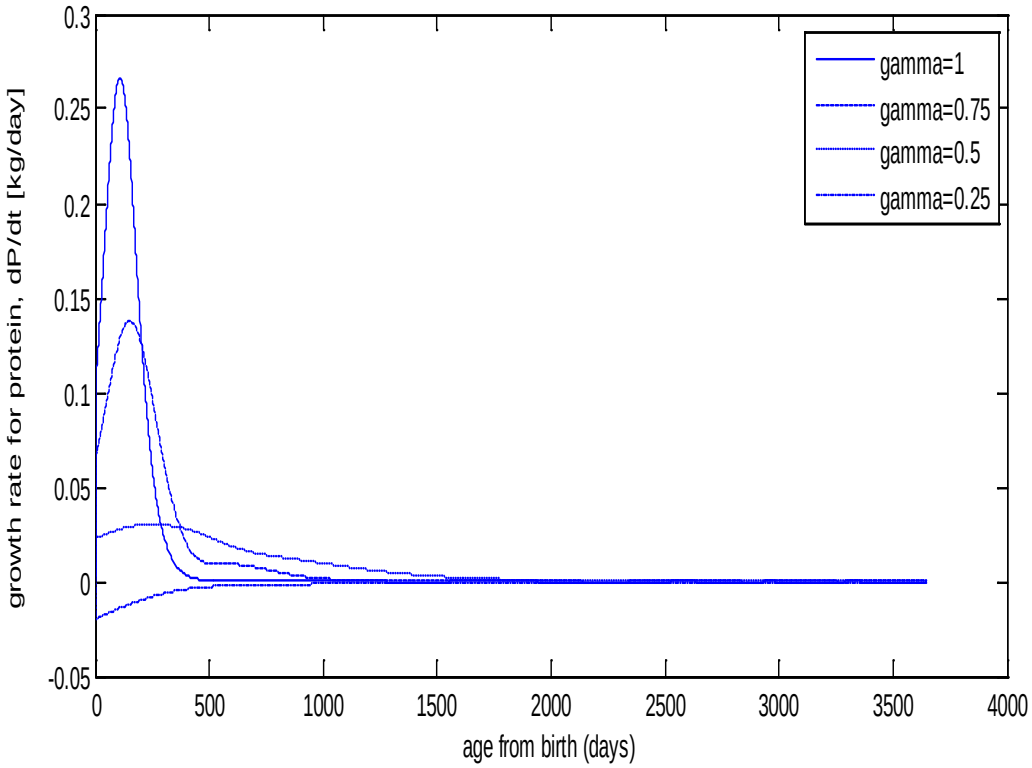

Figure 6.6: The growth rate for protein, $\frac{dP}{dt}$.

This graph (Figure 6.6) plots the growth rate of protein against time. It shows that the maximum peak in growth rates is slightly delayed by decreased feeding level. So, when $\gamma = 1$, we can see that the rate of change in protein in the first 100 days after birth is increasing at an incredibly rapid rate before reaching a maximum peak after which it decreases to zero. A growth rate of zero means that there is constant rate of protein growth in the animal. We can see that when $\gamma = 0.75$, it reaches its maximum a little later than when $\gamma = 1$ and it is not as high. However, we can also note that it takes longer for the protein growth rate to reach the steady state when we decreasing the value of γ (i.e. growth rate is equal to zero). There is also a significant change in growth rate for protein between

$\gamma = 0.5$ and $\gamma = 1$ (or even $\gamma = 0.75$). The growth rate is at its highest at the initial time and decreased from there. This means that the amount of protein in the animal's body receives, get less over time. It is interesting to note that when $\gamma = 0.25$, the curve of the graph is below *x*-axis (in the negative value) and then it starts to increase again. This indicates a warning sign to the animal that the animal is losing the protein and it should maintenance the protein in its body to survive. Eventually, the graph reaches a steady state at zero at which stage the change in growth rate for protein is constant. We can say that the model predicts that on high level of feeding ($\gamma = 1$), the peak growth occur from 12 to 16 weeks of age (with weight of 20- 30 kg) with an average empty-body gain in that time of 266.5g per day.

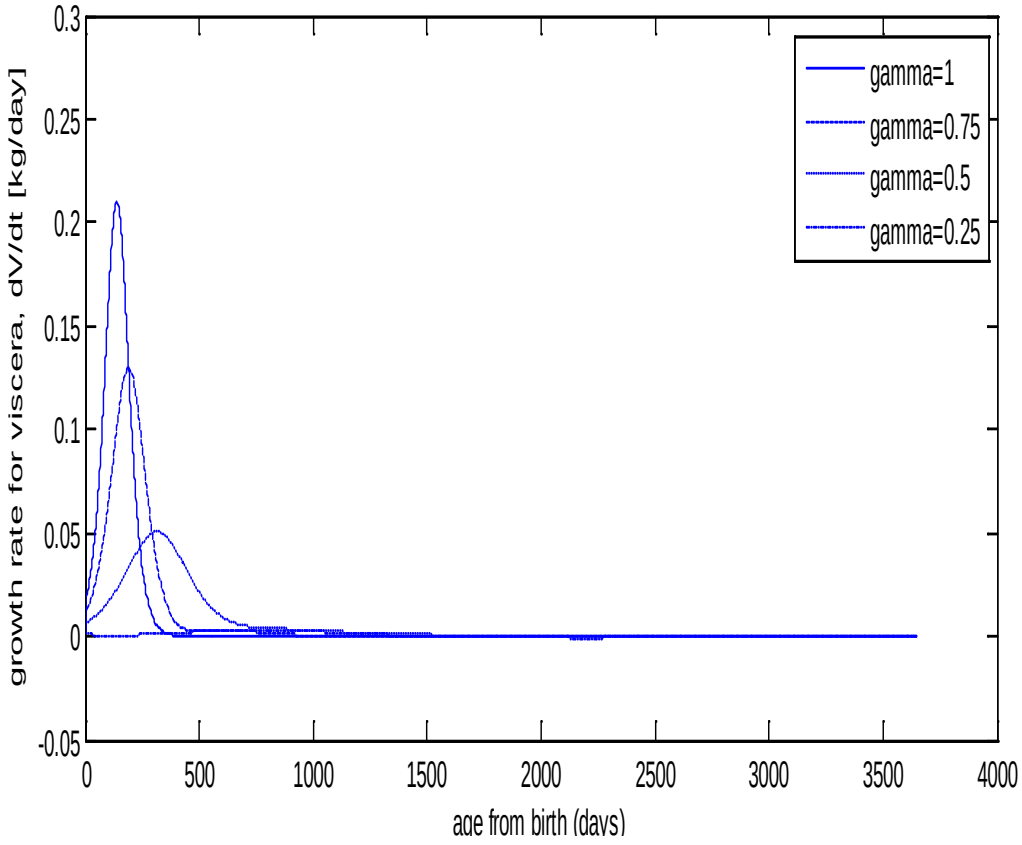

Figure 6.7: The growth rate for viscera, $\frac{dV}{dt}$.

For viscera (Figure 6.7), the peak growth occur from 17 to 20 weeks of age (with weight 10 – 15 kg) with average empty-body gain in that time of 210.3g per day.

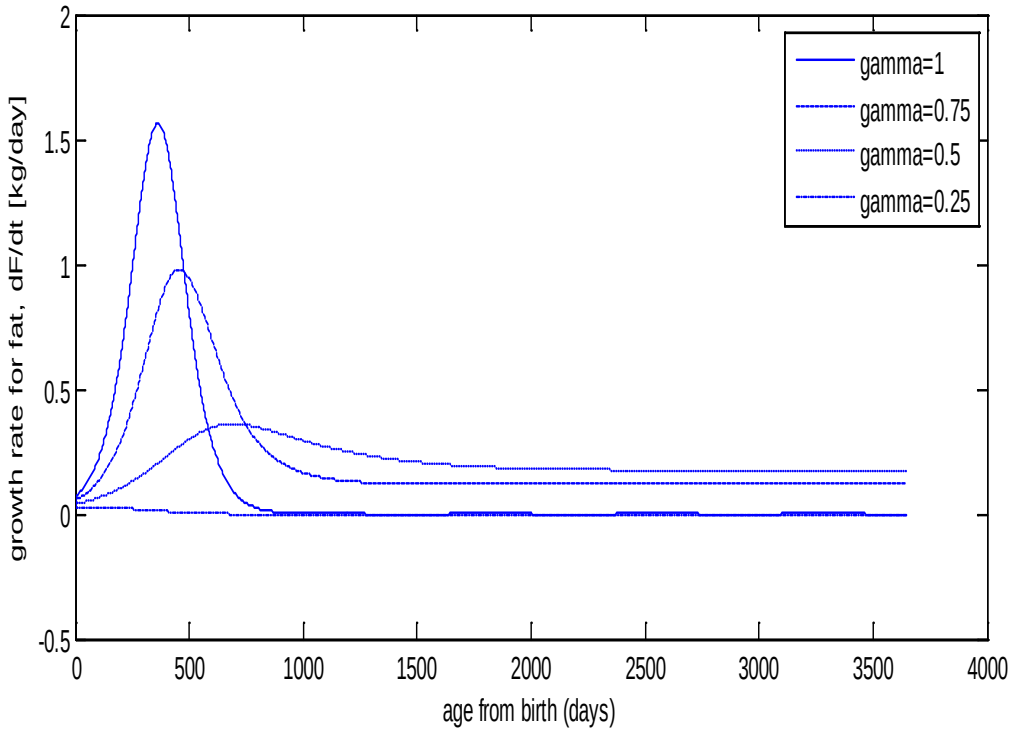

Figure 6.8: The growth rate for fat, $\frac{dF}{dt}$.

Meanwhile, the growth rate for fat (Figure 6.8) in the animal's body, the peak growth occurs from 50 to 52 weeks from birth (with 125 – 130 kg) with an average empty-body gain in that time of 1563g per day.

6.2.2 Structural Stability

A structural stability analysis is essential to establish the credibility of any model. It is rare for any model of physical situation to be exact; usually approximations have been made and often the values of the physical parameters are not exactly known. A structural stability analysis can throw a light on these issues by examining the effects of small changes in parameter values, establishing the generic behaviour predicted by the model and in particular, looking for any bifurcational change that may occur, implying qualitative changes in the behaviour of the real system.

As we can see from the previously section, the behaviour of this system is changing as we varied the feeding level, γ. We can say that this animal growth model has undergone bifurcation. These bifurcations are important as they provide models of transitions and instabilities as some control parameter is varied. We already provide a primer of the basic ideas and jargon of the bifurcation theory in Chapter 2. Our intent is to characterise the kinds of qualitative changes that may occur in this animal growth model as feeding level is changes. This includes the biochemical parameters changed after the re-parameterisation.

The analysis is carried out using path-following techniques that can reveal both stable and unstable solutions as a parameter is varied. To this end we construct a one-parameter bifurcation diagram, taking out the protein (P), viscera (V), fat (F) and nutrient (N) activities to represent the behaviour of the system and γ, the feeding level, as a particularly important, experimentally adjustable parameter. However, other continuation parameters could be chosen. The diagrams are created by software XPPAUT that has an interface of a powerful computer program AUTO.

(a)

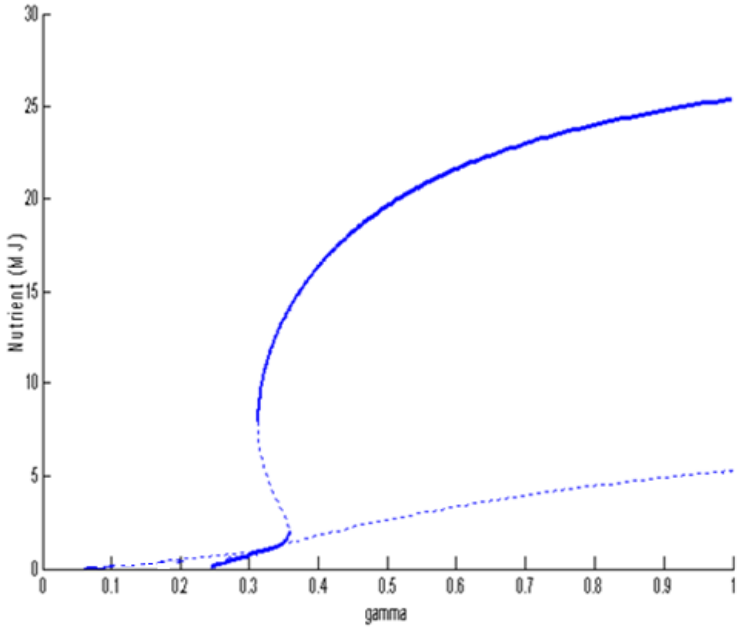
Nutrient (MJ)
gamma
0
5
10
15
20
25
30
0.1
0.2
0.3
0.4
0.5
0.6
0.7
0.8
0.9
1

(b)

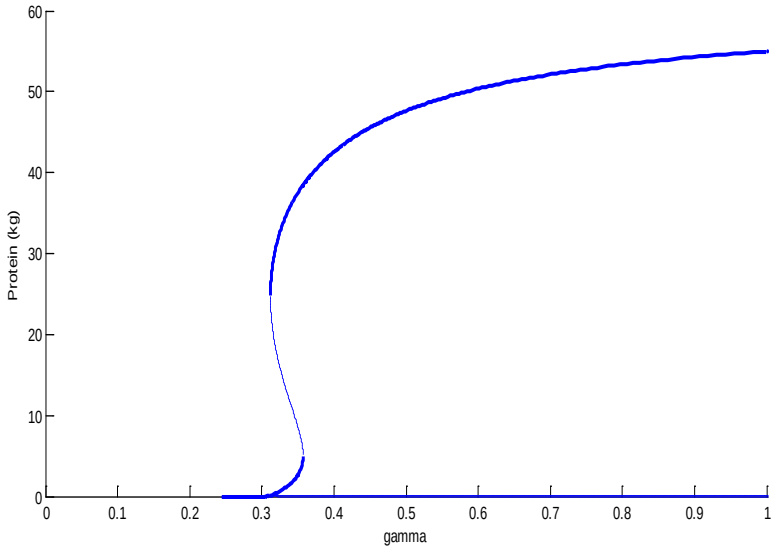
Protein (kg)
gamma
0
10
20
30
40
50
60
0.1
0.2
0.3
0.4
0.5
0.6
0.7
0.8
0.9
1

(c)

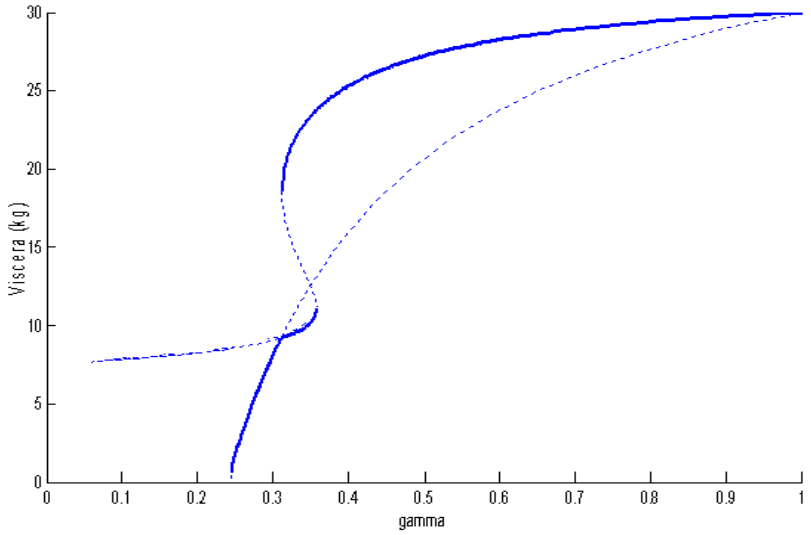

(d)

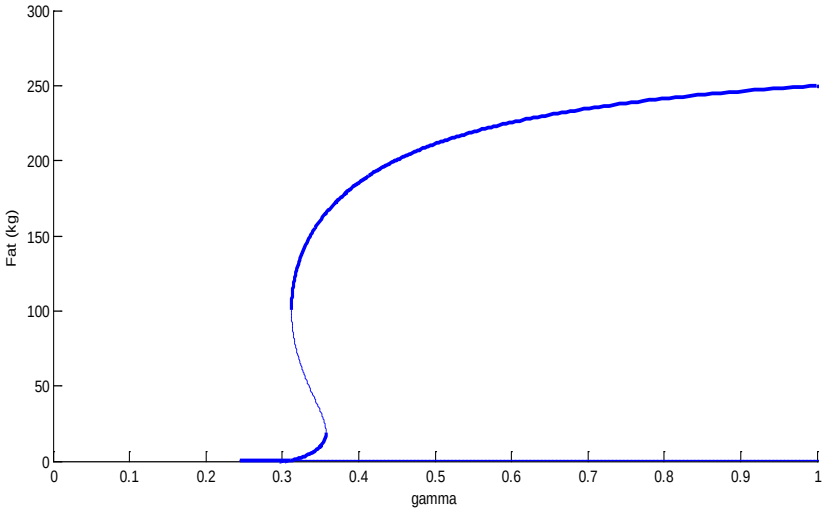

Figure 6.9: The steady state solutions (for nutrient (*N*), protein (*P*), viscera (*V*) and fat (*F*)) versus γ.

These figures (Figure 6.9) show the entire solution curve as the feeding level, γ is varied. The *y*-axis shows the steady state for each pool (*N*, *P*, *V* and *F*). These bifurcation

diagrams show a lot of remarkable points to note. The sold lines represent the stable steady states and the dashed lines represent unstable steady states.

This tells us how the animal's composition growth evolves in this model and which steady state they will tend towards. In the Figure (6.9a), we can see that the system for nutrient has two distinct (sometimes coexisting) stable solutions: a low and a high branch. For a small (high) γ, only the low (high) branch exists. Note that, in the range $0.312 < \gamma < 0.3573$, two qualitatively different stable states coexist. The existence of different stable states allows for the possibility of jumps and hysteresis as γ is varied. Suppose that we start the system in the state $N = 0$. There are two branches as we can see from the diagram, but we are interested in the stable one. Then, slowly we increase the value of γ. Then the state remains stable until $\gamma = 0.3573$, the steady state start losing its stability. Now, the slightest push of the value of *N* will cause the steady state to jump to the other stable branch. Same thing will happen if we start from the steady state at $\gamma = 1$ and decreasing the value of γ to get the state to jump back to the steady state $N = 0$. This lack of reversibility as a parameter is varied is call hysteresis.

In Figure (6.9b) it shows that when $\gamma = 0.2439$, the steady state $P = 0$ is stable and remain its stability until it reached $\gamma = 0.3573$. At that point of γ, the steady state becomes unstable. And just like in nutrient, there is a possibility of hysteresis and a delayed return to the normal state when γ is varied. The same situation happened in fat (see Figure 6.9d).

There is something interesting and different diagram for state variable viscera (*V*) (Figure 6.9c). It shows that there are two different branches which did not intersect but this happened because four variables (i.e. *P*, *V*, *F* and *N*) collapsed onto two variables. If we start the $\gamma = 0.2439$, the steady state for viscera is stable until it reach $\gamma = 0.3108$, it change the stability. In other branch, the lower γ is unstable but it changes to become stable until $\gamma = 0.3108$ and change the stability to unstable at $\gamma = 0.3573$. If we start from a higher value of γ, the steady state is stable until it reach the limit point at $\gamma = 0.312$ become unstable. Between the range $0.312 < \gamma < 0.3573$, there is a possibility of jump and hysteresis to happen. Figures 6.9(a) and 6.9(c), it seems to be there is a bifurcation point in the diagram but actual it is not. If we try to plot the bifurcation diagram in *N*, *P*, *V*, *F*, γ – space (i.e. in five-dimensional), the two branches will eventually join.

From the bifurcation diagram for protein (*P*) (Figure 6.9b), we can see that if we take the value of γ between range $0.312 < \gamma < 0.3573$, there is a multiple stability of the steady state solutions. There is a "watershed region" within that range. Watershed implies an important boundary for the basin of stability of the two stable steady states. That is, the initial condition determines which steady state the transient solution approaches in large time. For multidimensional system, this watershed is not simply the intermediate unstable steady state.

Now, let us give a simple example in one-dimensional that illustrate the unstable intermediate steady state which is the watershed region.

Consider,

$$\frac{dx}{dt} = -x(1-x)\left(1-\frac{x}{2}\right) \tag{6.3}$$

$$\frac{dx}{dt} = -x + \frac{3}{2}x^2 - \frac{1}{2}x^3 .$$

Then, the steady state points are $x = 0,1,2$.

To determine the stability of this steady state points, find the derivatives of the equation by letting $f(x) = \frac{dx}{dt}$.

$$f'(x) = 1 + 3x - \frac{3}{2}x^2 \tag{6.4}$$

Steady state points	$f'(\bar{x})$
$\bar{x} = 0$	$-1 < 0$ stable
$\bar{x} = 1$	$\frac{1}{2} > 0$ unstable
$\bar{x} = 2$	$-1 < 0$ stable

Table 6.3: The stability of the steady state points

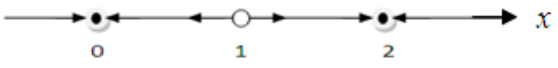

Figure 6.10: The phase portrait for $\frac{dx}{dt} = -x(1-x)\left(1-\frac{x}{2}\right)$.

It shows that if we take the initial value less than 1, the solution will shift down and tends to the nearest stable steady state which is at $x_s = 0$. Same if we take the initial value larger than 1, it will move towards the nearest steady state at $x_s = 2$.

Now, we try to illustrate this example in this animal growth model. Let say we take the intermediate value of γ at $\gamma = 0.3337$. So, there are three different values of steady state protein which two of them are stable ($P_1$and P_3) and another one is unstable (P_2). We tried to plot the solution trajectories for steady state P at $\gamma = 0.3337$.

P_s	Value	Stability
P_1	1.134	Stable
P_2	13.42	Unstable
P_3	34.35	Stable

Table 6.4: The values of the steady state of protein at $\gamma = 0.3337$.

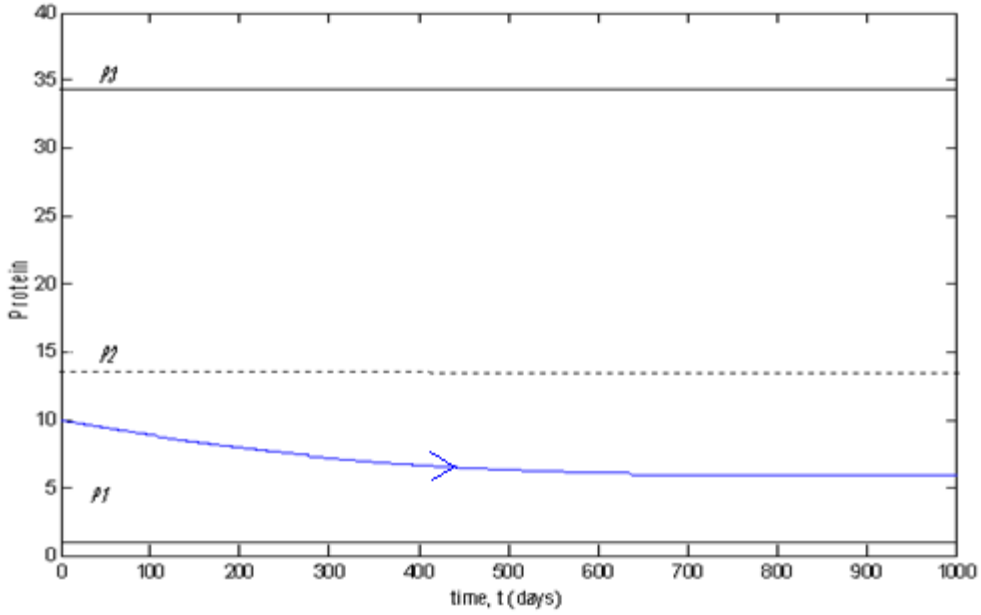

Figure 6.11: The multiple steady states of protein at $\gamma = 0.3337$ where the solid lines are stable and the dashed line is unstable. The arrow line is the projection when the initial value is less than the P_2 (unstable steady state).

It shows that in Figure 6.11, when the initial value of $P(0) < P_2$, the growth in protein decreases with time and asymptotically approaches the nearest stable steady state P_1. We can say that if the initial values of P is disturbed slightly before P_2, the disturbance will decay monotonically and $P(t) \to P_1$ as $t \to \infty$. But it is an interesting and different case when the initial value of $P(0) > P_2$, it crosses the intermediate unstable steady state P_2 as time increases (Figure 6.12). It must be remembered that we have here fixed the initial value of $V(0) \sim V_2$ and $F(0) \sim F_2$ (where V_2 and F_2 are the unstable steady state values at $\gamma = 0.3337$). This is not the same in the one-dimensional case that we have just illustrated where we expect that the trajectory should be move towards the nearest stable steady state P_3. In the Figure 6.12, it shows that at some points of $P(0)$, it does not crosses the unstable

P_2 line. On the contrary, when we set the initial values of $V(0)$ and $F(0)$ as $V(0) << V_2$ and $F(0) >> F_2$, respectively, the trajectories move up towards the stable steady state P_3 (Figure 6.13). We can conclude that the basin of the stability is not uniquely determined by the intermediate unstable steady state. The steady state response diagrams (Figure 6.9) does not easily show what the watershed value of $P(0)$ actually is. Also the initial values of the other state variables (i.e. N, V and F) will affect the long-term outcome. These reveal that the implications on the initial conditions at birth of the body composition will determine which steady state the animal will approach as it matures. The watershed for this system is complicated as the system is in five-dimensional space (i.e. (N, P, V, F, γ)- space) rather than the simple one that we already seen in just one-dimensional. Also, we can say that the intermediate unstable steady state for all the variables (i.e. N_2, P_2, V_2 and F_2) is not the true boundary for the watershed.

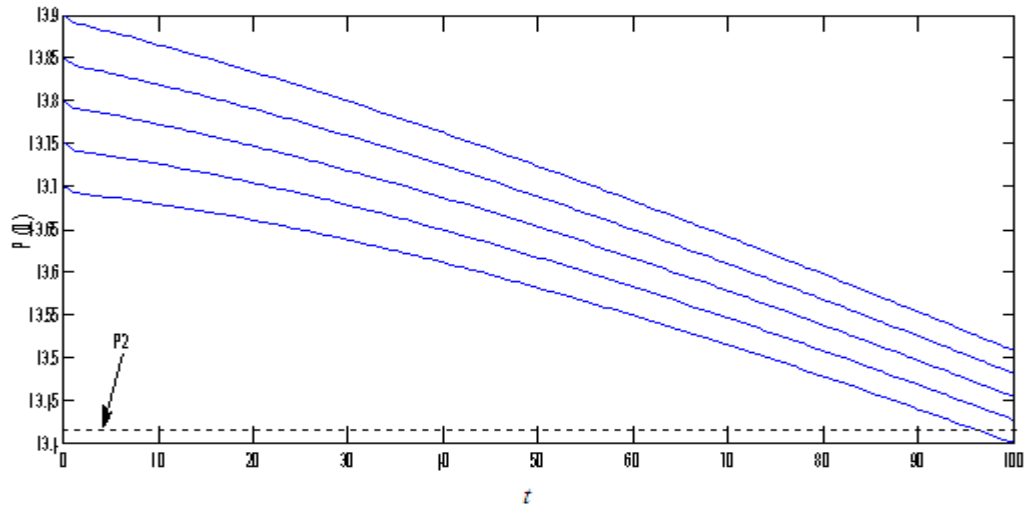

Figure 6.12: The projection of protein when initial values of protein, $P(0)$, is varied but fixed the value of $V(0) \sim V_2$ and $F(0) \sim F_2$.

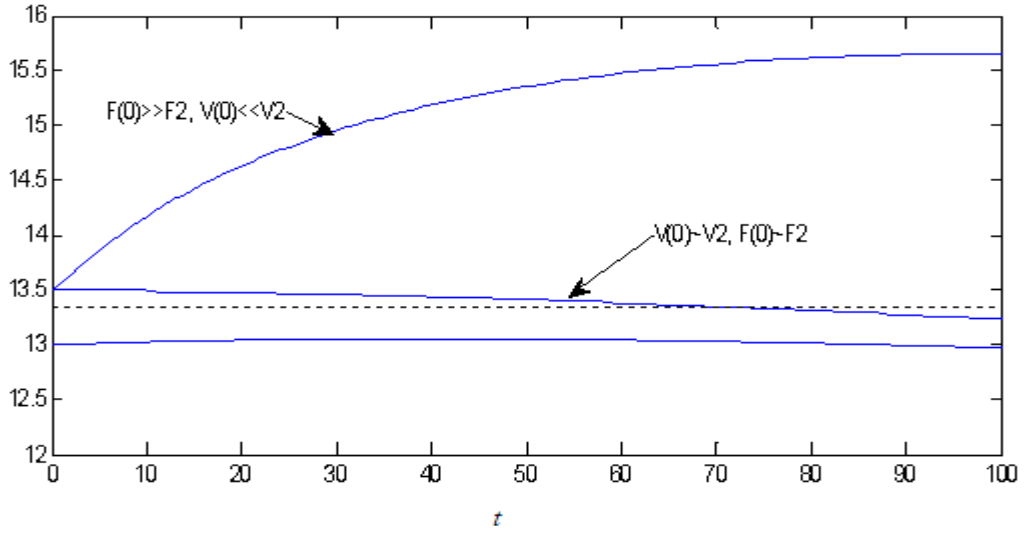

Figure 6.13: The projection of protein near the intermediate value of P_2 (the dashed line).

6.2.3 Phase Space

A phase-space diagrams are useful tool in studying dynamical system. They consist of a plot of the solution trajectories in the one state space. Consequently, we are able to draw some general conclusion about the model and to verify the observations which have been made.

Recall that the equations for this animal growth model are:-

$$\frac{dN}{dt} = I_I + I_{KP} + I_{KV} + I_{KF} - I_{AP} - I_{AV} - I_{AF} - I_E$$

$$\frac{dP}{dt} = \frac{1}{\rho_P}(I_{AP} - I_{KP})$$

$$\frac{dV}{dt} = \frac{1}{\rho_V}(I_{AV} - I_{KV})$$

$$\frac{dF}{dt} = \frac{1}{\rho_F}(I_{AF} - I_{KF})$$

We can say that the solutions have trajectories in a 4-dimensional space where in the phase space $\{(N(t), P(t), V(t), F(t)) : t > 0\}$. Obviously, it is a difficult task to draw a 4-diemnsional phase space. Therefore, we tried to plot the planar projections of the phase space for this animal growth model.

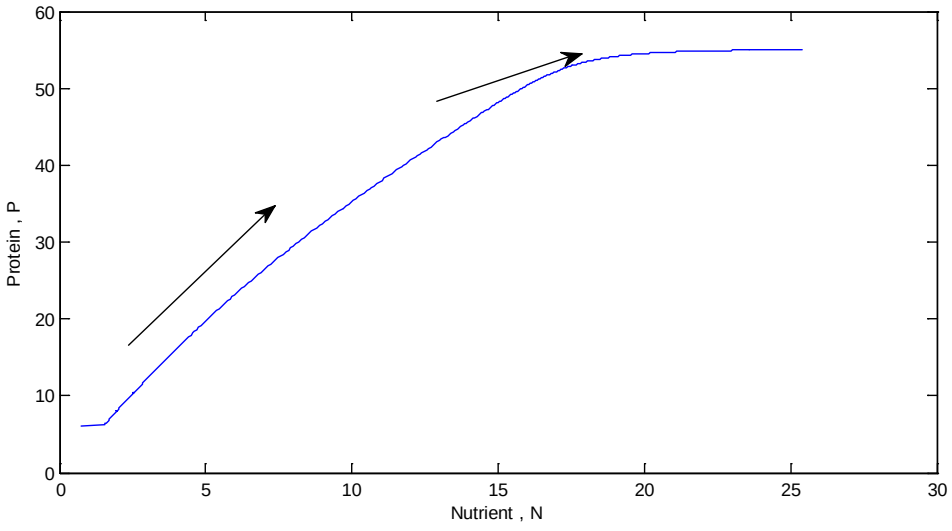

Figure 6.14: The phase space diagram for nutrient and protein.

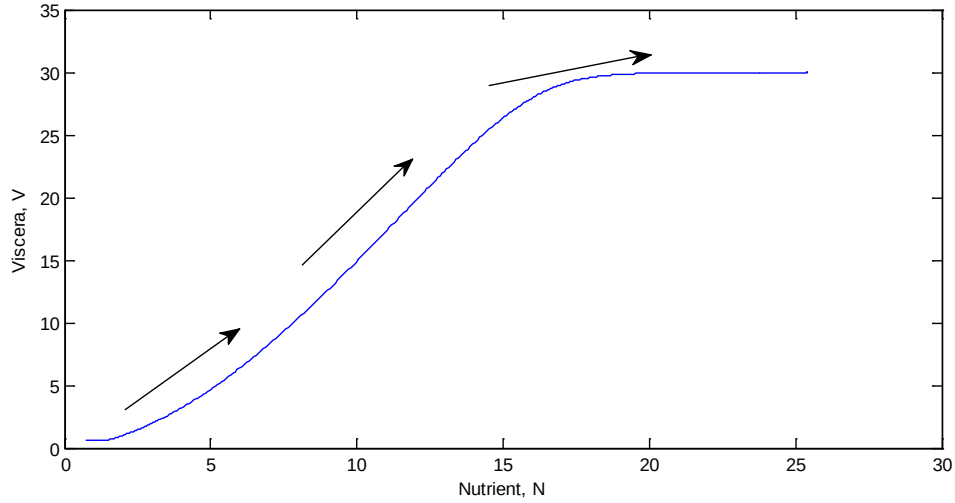

Figure 6.15: The phase space diagram for nutrient and viscera.

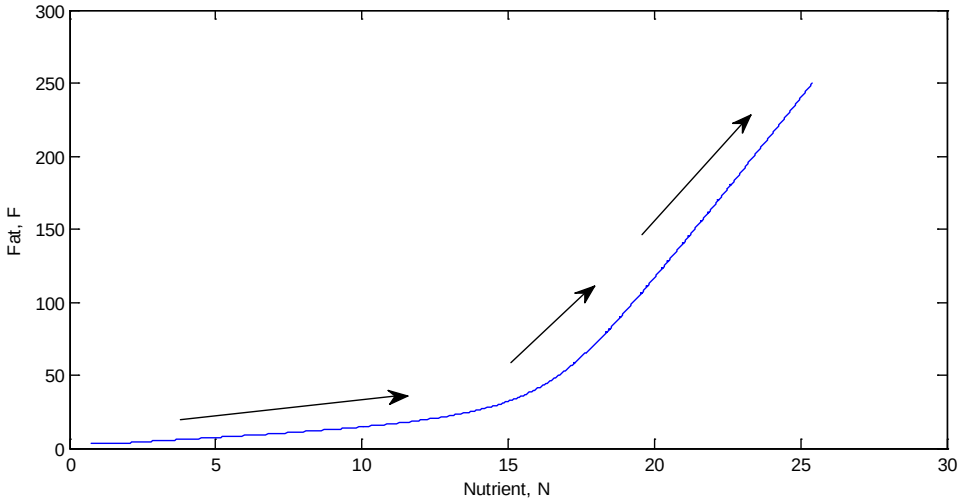

Figure 6.16: The phase space diagram for nutrient and fat.

6.3 Biological Interpretation

Many relationships are available to predict feeding level by ruminant. These are generally deterministic in which the feeding level will be a function of the animal's hormonal and neural responses to its energy status or demand. For this animal growth model proposed by Oliviera *et al*, the feeding level will be a function of the body composition (i.e. nutrient, protein, viscera and fat).

During evolution of this animal growth model, it was apparent that rates of change in body composition were predicted when changes in feeding level occurred (refer to the figures in Section 6.2.1). If given at the highest level of γ, the animal's growth is increases. In contrast, the animal fed at lower γ, lose weight rapidly as body composition (i.e. protein, viscera and fat) is catabolised. The animal's growth continues to increase for the remainder of the time; over the same period, the animal that is fed a restricted ration loses weight continuously, but a declining rate.

The feeding level is subject to deterministic control, but if it is non-linear, the process could be chaotic. This of course means that the feeding level could be modelled within certain bounds, as the trajectory would be sensitively dependent on initial conditions of the body composition. This can be proved by the bifurcation diagrams shown in Figure 6.9. For low or high values of γ the system has one stable steady state. However, the intermediate values of γ the system have three steady states namely two stable steady states and one unstable. There are possibilities of jump and hysteresis at certain range of feeding level, γ. This was determined by the initial conditions of the body composition in the

animal at birth. From this knowledge, it will tell us to which steady state the animal will approach when it tends to maturity.

CHAPTER 7

CONCLUSIONS AND FURTHER WORK

This animal growth model proposed by Oliviera *et al* provides a description of animal growth which is derived from dynamic principle of growth based on the energy fluxes. The main objective of this project was the investigation in growth response to controlled feeding level. Feeding level, γ, is the ratio of the absorbed energy intake versus demand. The model performed well in describing the dynamics and energetic of growth, from conception and maturity, both qualitatively and quantitatively. It shows that there is a transient growth when the level of food intake is varied. This will give useful information e.g. for planning feed supply and strategies or in forecasting average animal performance.

Mathematically, this animal growth model has a multiple steady state at the intermediate range of the value γ. When we tried to plot the one-parameter bifurcation diagram, it produced an interesting subcritical pitchfork bifurcation. Where there exists a possibility of jump and hysteresis at certain range of feeding level, γ. This is because the trajectory is sensitively dependent on the initial conditions of the animal's body composition such as protein, viscera and fat. Moreover, the watershed for this animal growth system is complicated as they were in the five-dimensional space.

This project is a ‘stepping-stone’ to explore the stability of the model proposed by Oliviera *et al*. This model has been specifically formulated the necessary criteria of the animal growth specifically for dairy cows. We consider here how to continue from the work laid out in this thesis. One should use other parameters that can be control and do the analysis of the two or more-parameter bifurcation diagram. At the same time change some of the other parameter values. Besides that, the analysis will be interesting if one can connect the model’s behaviour before and after parameterization by using the theory of homotopy-variations.

REFERENCES

Allen, M.S. & Bradford, B.J. (2005). Energy Partitioning and Modelling in Animal Nutrition. *Annu. Rev. Nutr*. **25**. 523-547.

Alligood, K.T., Sauer, T.D., & Yorke, J.A.. (1996). *Chaos: An Introduction to Dynamical Systems.* Springer. USA.

Baldwin, R.L. (1995). *Modelling Ruminant, Digestion and Metabolism.* Chapman & Hall. UK.

Baldwin, R.L. & Sainz R.D. (1995). Energy Partitioning and Modelling in Animal Nutrition. *Annu Rev. Nutr*. **15**. 191-211.

Barnes, B. & Fulford, G.R. (2002). *Mathematical Modelling with Case Studies. A Differential Equation Approach Using Maple*. Taylor & Francis. USA.

Blaxter, K.L. (1962). *The Energy Metabolism of Ruminants*. Hutchinson & Co. UK.

Braza, P.A. (2003). The Bifurcation Structure of the Holling-Tanner Model for Predator-Prey Interactions Using Two-Timing. *SIAM J. Appl. Math*. **63**. 3. 889-904.

Crawford, J. D. (1991). Introduction to Bifurcation Theory. *Rev. Mod. Phys*. **63**. 4. 991-1037.

Ellner, S.P. & Guckenheimor, J. (2006). *Dynamic Models in Biology*. Princeton University Press. USA.

Ermentrout, B. (2002). *Simulating, Analyzing, & Animating Dynamical Systems; A Guide to XPPAUT for Researches and Students.* SIAM.

France, J. & Kebreab, E. (2008). *Mathematical Modelling in Animal Nutrition*. C.A.B. International. UK.

Freetly, H. L. (1995). Dynamics of Liver and Viscera Metabolism. *Modelling Ruminant, Digestion and Metabolism.* Chapman Hall. UK.

Jones, D.S. & Sleeman, B.D. (2003), *Differential Equations and Mathematical Biology*. Chapman & Hall. USA.

Lynch, S. (2004). *Dynamical Systems with Applications Using Matlab*. Birkhauser. USA.

McDonald, P., Edwards, R.A., Greenhalgh, J.F.D., & Morgan, C.A., (2002). *Animal Nutrition.* 6th Edition. Pearson Education Limited. UK.

Oddy, V.H. & Ball, A.J. & Pleasants, A.B. (1997). Understanding Body Composition and

Efficiency in Ruminants: *A Nonlinear Approach Recent Advances in Animal Nutrition in Australia.*UNE Armidale, Australia. 209-222.

Oltjen, J.W., Pleasant, A.B., Soboleva, T.K., & Oddy, V.H. (2000). Second-Generation Dynamic Cattle Growth and Composition Model. *Modelling Utilization in Farm Animals*. C.A.B. International, UK. 197-209.

Oltjen, J.W., Sainz, R.D., Pleasant, A.B., Soboleva, T.K., & Oddy, V.H. (2006). Representation of Fat and Protein Gain at Low Levels of Growth and Improved Prediction of Variable Maintenance Requirement in a Ruminant Growth and Composition Model. *Nutrient Digestion and Utilization in Farm Animals: Modelling Approaches.* 144-159. C.A.B. International. UK.

Oltjen, J. W. & Sainz, R.D. (1995). Mechanistic and Dynamic Models of Growth. *Modelling Ruminant, Digestion and Metabolism*. Chapman Hall. UK.

Parks, J.R. (1982). *A Theory of Feeding and Growth of Animals*. Springer-Verlag. NY.

Schaefer, A.L. & Krishnamurti, C.R. (1984). Whole Body Tissue Fractional Protein Synthesis in the Ovine Fetus in Utero. *British Journal of Nutrition*. **52**. 359-369.

Strogatz, S. H. (1994). *Studies in Nonlinearity; Nonlinear Dynamics and Chaos: With Applications to Physics, Biology, Chemistry, and Engineering*. Perseus Book.

Suttie, J. M. & Webster, J. R. (1995). Extreme Seasonal Growth in Arctic Deer: Comparisons and Control Mechanism. *American Zoologist*. **35**. 215-221.

Tabor, M. (1989). *Linear Stability Analysis Chaos and Integrability in Nonlinear Dynamics: An Introduction.* NY. Wiley. 20-31.

Temme, N. M. (ed). (1978). *Nonlinear Analysis*. Vol. I . MC Syllabus 26.1 . Amsterdam.

Thornley, J.H.M. & France, J. (2005). An Open-ended Logistic-Based Growth Function. *Ecological Modelling*. **184.** 257-261.

Thornley, J.H.M, & France, J. (2007). *Mathematical Models in Agriculture.* 2nd Edition. C.A.B. International. UK.

Tucker, H. A. (1996). Photoperiodic Regulation of Growth. *Proceedings of Scientific Conference on Growth Promotion in Meat Production, Brussels 1995*. Commission of the European Communities. Luxemborg.

Vetharaniam, I., McCall, D.G., Fennesy, P.F. & Garrick, D.J. (2001a). A Model of Mammalian Energetics and Growth: Model Development. *Agricultural Systems*. **68.** 55-68.

Vetharaniam, I., McCall, D.G., Fennesy, P.F. & Garrick, D.J. (2001b). A Model of Mammalian Energetics and Growth: Model Testing (Sheep). *Agricultural Systems*. **68.** 69-91.

Wickham, I. (1997). *Dynamical Systems Models of the Protein Pool in Animal Growth*. Master Thesis. University of Auckland.